Stress interaction between seismic and volcanic activity at Mt Etna

Nathalie Feuillet, Massimo Cocco, Carla Musumeci, Concetta Nostro

Stress interaction between seismic and volcanic activity at Mt Etna

Nathalie Feuillet,[1,*] Massimo Cocco,[1] Carla Musumeci[2] and Concetta Nostro[3]

[1] *Istituto Nazionale di Geofisica e Vulcanologia, Department of Seismology and Tectonophysics, Rome, Italy*
[2] *Istituto Nazionale di Geofisica e Vulcanologia - Sezione di Catania, Catania, Italy*
[3] *Istituto Nazionale di Geofisica e Vulcanologia, Centro Nazionale Terremoti, Rome, Italy*

SUMMARY

Mt Etna lies on the footwall of a large normal fault system, which cuts the eastern coast of Sicily and crosses the volcano eastern flank. These faults are responsible for both large magnitude historical earthquakes and smaller damaging seismic events, closer to the volcano. We investigate here the two-way mechanical coupling between such normal faults and Mt Etna through elastic stress transfer. The comparison between eruptive sequences and historical seismicity reveals that the large earthquakes which struck the eastern Sicily occurred after long periods of activity along the Mt Etna rift zone. The larger the erupted lava volumes, the stronger the earthquake. The smaller earthquakes located on the eastern flank of the volcano occur during periods of rift zone eruptions. We point out that the seismicity rates are well correlated with the rate of erupted lava. By modelling elastic stress changes caused by earthquakes and eruptions in a 3-D elastic half-space, we investigate their interaction. Earthquake dislocations create a vertical stress gradient along fissures oriented perpendicular to the minimum compressive stress and compress shallow reservoirs beneath the volcano. This may perturb the magmatic overpressures in the Etna plumbing system and influence the transport and storage of the magma as well as the style of the eruptions. Conversely, the large rift zone eruptions increase up to several tenths MPa the Coulomb stress along the eastern Sicily normal fault system and may promote earthquakes. We show that the seismic activity of the normal faults that cut the eastern flank of the volcano is likely to be controlled by Coulomb stress perturbations caused by the voiding of shallow reservoirs during flank eruptions.

Key words: Coulomb stress modelling, earthquakes–volcanoes interaction, historical eruptions, Mt Etna, stress transfer.

GJI Volcanology, geothermics, fluids and rocks

1 INTRODUCTION

Investigating the mechanical coupling between earthquakes and eruptions is very important to better assess the seismic and volcanic hazard in highly exposed and populated regions. Time correlations between these two phenomena have been observed in numerous regions of the world (e.g. Nostro *et al.* 1998; Hill *et al.* 2002, and references therein). Several studies have shown that static stress changes imparted by the volcano to faults and by the earthquakes to the volcanoes may have promoted seismic events and volcanic eruptions. Volcanic processes are able to promote earthquakes along neighbouring faults by increasing the Coulomb stress. Similarly, a volcanic system, which has reached a critical state, can be perturbed by small stress changes caused by a large earthquake occurred nearby (see Hill *et al.* 2002, and references therein). In Italy, Nostro *et al.* (1998) have shown that large normal faulting earthquakes along the

Apennines promoted Vesuvius eruptions by compressing the magmatic chamber at depth and by opening suitably oriented dikes at the surface. In Japan, Toda *et al.* (2002) have shown that dike opening at Izu island promoted $M \geq 6$ strike-slip earthquakes, tens of kilometres from the volcano. In Hawaii, Cayol *et al.* (2000) have pointed out that earthquakes occurring far from the Kilauea rift zone were promoted by Coulomb stress changes caused by the dilation of the rift zone during the large 1983 flank eruption. Walter & Amelung (2004) have calculated the Coulomb stress changes caused by volcanic activity at Mauna Loa (Hawaii) on the Kaoiki seismic zone; they show that earthquake occurrence is influenced by volcanic eruptions. In Djibouti, Jacques *et al.* (1996) showed that the distribution of the seismicity recorded for several months after the 1978 eruption in the Asal rift may be explained by the pattern of Coulomb stress perturbations generated by the opening of eruptive dikes.

We investigate this two-way mechanical coupling at Mt Etna for two main reasons. First, because of the excellent historical data, with exceptionally long catalogues. Second because the tectonic context of the volcano, which is located on the footwall of a large normal

---

*Now at: Institut de Physique du Globe de Paris, France.
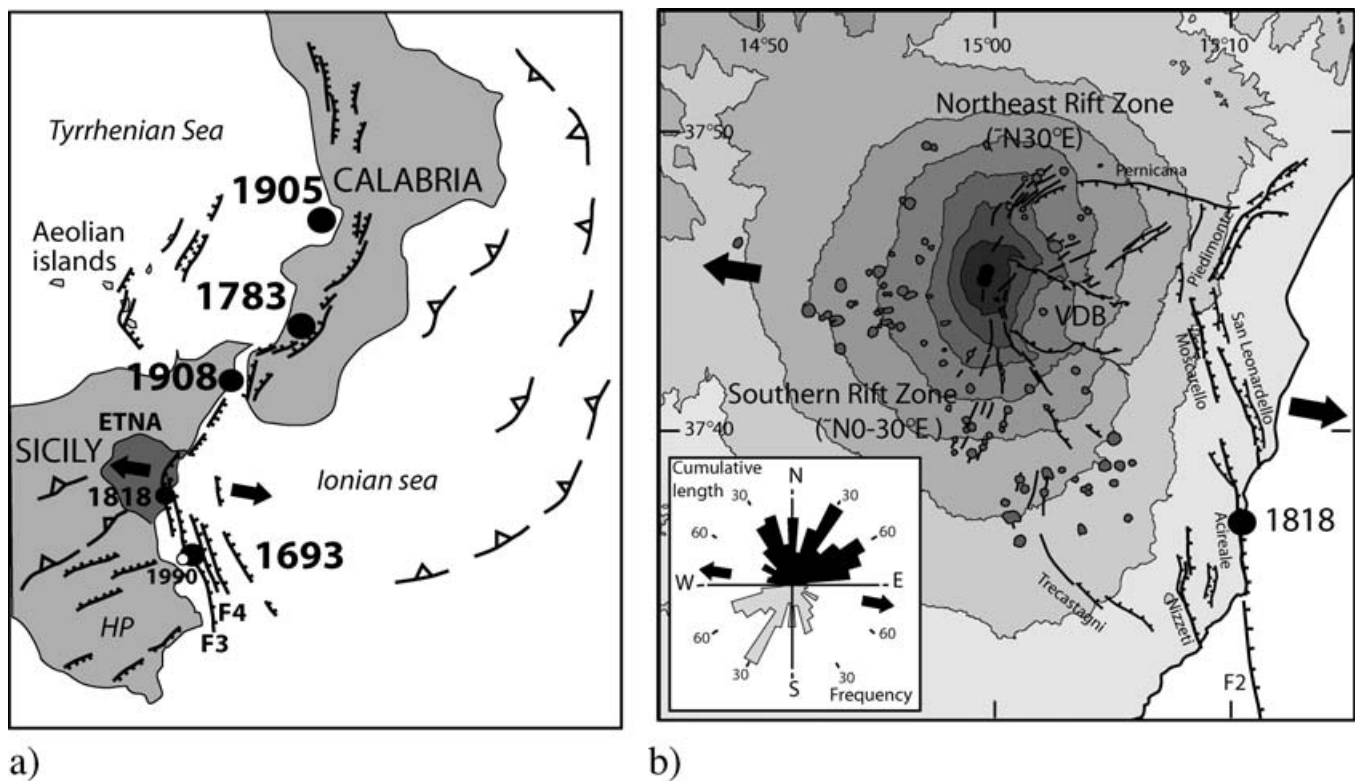E-mail: feuillet@ipgp.jussieu.fr

Figure 1. (a) Largest earthquakes since 1600 A.D. and active faulting in Calabria and eastern Sicily (modified from Monaco *et al.* 1997). Normal faults offshore from Hirn *et al.* (1997) and Nicolich *et al.* (2000), HP: Hyblean plateau. Black arrows: direction of extension (from Monaco *et al.* 1997) (b) Active faults and eruptive dikes (rift zones) at Mt Etna (modified from Monaco *et al.* 1997). Eruptive cones in grey. VDB: Valle Del Bove. Black arrows as in Fig. 1(a). Black circle: location of the 1818 earthquake from Azzaro & Barbano (2000). Inset: diagram showing the distribution of the eruptive dikes in function of their strike (cumulative length and frequency) from Rasà *et al.* (1982).

fault system cutting the eastern shore of Sicily, is well known (Fig. 1 and Monaco *et al.* 1997; Hirn *et al.* 1997; Azzaro & Barbano 2000). Ellis & King (1991) have illustrated, through 2-D boundary element models, the tectonic coupling between normal faults and volcanoes located on their footwall. They have shown that slip on normal faults is able to generate an extensional strain field at the base of their footwall, allowing the opening of dikes and further transport of magma towards the surface by hydro-fracturing. Monaco *et al.* (1997) proposed that the Etna's magmatism can be a consequence of such a process, implying a strong coupling between faulting and volcanism at Mt Etna.

In this study, we model the Coulomb stress changes caused by Etna eruptions on the Sicilian normal faults as well as the normal and volumetric stress changes generated by large earthquakes on the Etna plumbing system. We have first analysed the historical catalogues of the eruptions (Romano & Sturiale 1982; Acocella & Neri 2003; Branca & Del Carlo 2004), sorting out the summit and flank eruptions and mapping each eruptive fissure on the Etna digital elevation model. Then, we have compared the sequence of eruptions and the occurrence of the largest earthquakes in the eastern Sicily to investigate the temporal evolution and the correlation between these two phenomena. The analysis of the database of small-to-moderate earthquakes compiled by Azzaro *et al.* (2000, 2002) allowed us to compare the seismic activity along the eastern Sicily normal fault system, where it crosscuts the Mt Etna flank (Fig. 1b), with the volcanic activity. In the following sections we will describe the most relevant features of the seismicity of the eastern Sicily and eruptions at Mt Etna in order to point out their temporal correlations and to model their interaction through elastic stress transfer.

2 EASTERN SICILY EARTHQUAKES

Eastern Sicily is characterized by several distinct tectonic regimes. The Hyblean plateau deforms in response to the NNW convergence of the European and African plates (Musumeci *et al.* 2005), whereas the eastern coast of Sicily is cut by NE–NNW-striking, east-dipping normal faults that form a narrow extensional zone between the Messina strait and the southern shore of Sicily (see Fig. 1a and Monaco *et al.* 1997; Hirn *et al.* 1997; Bianca *et al.* 1999). This system extends farther south in the Ionian plain along the Malta escarpment (Azzaro & Barbano 2000).

Large earthquakes ($M \sim 7$) struck eastern Sicily on 1169 February 4, on 1693 January 11 and on 1908 December 28 (see Fig. 1a and Baratta 1901; Boschi *et al.* 1995). The 1908 December 28 event occurred along normal faults in the Messina strait (e.g. Boschi *et al.* 1989). Another large event occurred close to Mt Etna, on 1783 February 5, along NNW-striking faults, in Southern Calabria (e.g. Jacques *et al.* 2001). The sources of the oldest 1169 and 1693 events are still debated and different fault models have been proposed. For the 1693 earthquake some authors, relying on the distribution of macroseismic intensities, propose an inland rupture along a NNE–SSW strike-slip fault cutting the Hyblean plateau (e.g. Boschi *et al.* 1995; Sirovich & Pettenati 1999). Others (e.g. Hirn *et al.* 1997; Piatanesi & Tinti 1998; Bianca *et al.* 1999; Azzaro & Barbano 2000) argue that it occurred offshore in the Gulf of Catania on the normal fault system that follows the Malta escarpment along the Ionian coast (faults F3 or F4 of Hirn *et al.* 1997, see Fig. 1a). Azzaro & Barbano (2000) suggest that the 1169 and the 1693 earthquakes ruptured the same fault system. This fault system cuts across the Mt Etna

eastern flank through the Acireale–Piedimonte normal faults (see Fig. 1b and Monaco *et al.* 1997). At this place, it produced smaller and shallower earthquakes as commonly observed around volcanic areas. The largest event reported along the Acireale–Piedimonte faults occurred on 1818 February 20, and reached magnitude 6. It caused damages on eastern flank of Mt Etna and was felt on the whole of Sicily (e.g. Baratta 1901; Azzaro 1999; Azzaro & Barbano 2000). The most important earthquake ($M = 5.4$) that struck the eastern coast of Sicily since 1818 occurred on 1990 December 13 offshore Brucoli near the Malta escarpment (Amato *et al.* 1995).

3 ETNA ERUPTIONS

Mount Etna's main eruptive system consists of N30°E to 160°E-striking rift zones parallel to the Acireale–Piedimonte faults and probably originating from the same extensional stress field (e.g. Fig. 1b and Monaco *et al.* 1997). As in many large basaltic volcanoes, the volcanic products erupt either in the summit area or along rift zones at large horizontal distances from the summit crater and storage zones (see Figs 2 and 3, and Lister & Kerr 1991). Recently, Behncke & Neri (2003) showed that, although Mt Etna erupts almost continuously, it has a cyclic behaviour at the scale of decades and probably centuries. The short-term cycles (decades) are characterized by three phases of activity: a period of inactivity (few years), a period of summit eruptions and finally a period of flank eruptions, with the largest volume of erupted lava. The largest known flank eruptions of Mt Etna, with ∼3 km³ of erupted products and a high mean output rate of ∼1.5 m³ s⁻¹ occurred during the 17th century, between 1600 and 1669 (Fig. 4). The 1669 eruption is of interest

in terms of volcanic hazard since it destroyed part of the city of Catania (Boschi & Guidoboni 2001). After 1669, the volcanic activity drops sharply (see Fig. 4) reaching the lowest recorded output rate (<0.03 m³ s⁻¹). By comparison with short-term eruptive cycles, Behncke & Neri (2003) suggest that these huge flank eruptions may correspond to the end of a longer-term cycle on the scale of centuries.

This cyclic behaviour may be controlled by magma supply rates in the reservoir as shown in fluid-dynamic models by Meriaux & Jaupart (1995). These models reveal that when the magma is supplied at high rates in a reservoir, summit eruptions are likely to occur as a result of failure above the injection point. However, when the magma supply rate decreases, the reservoir pressure drops and the magma is likely to be injected in fissures or rift zone dikes.

4 TIME CORRELATION BETWEEN EARTHQUAKES AND ERUPTIONS

Several studies have looked for a link between volcanic and seismic activity at Etna volcano (Sharp *et al.* 1981; Nercessian *et al.* 1991; Gresta *et al.* 1994; De Rubeis *et al.* 1997; Hirn *et al.* 1997). Sharp *et al.* (1981) and Nercessian *et al.* (1991) performed statistical analyses using all eruptions and seismic events that occurred since 1582 within 200–300 km of the volcano, independent of their tectonic origin and magnitude. Depending on how they select the events, these authors obtained different results. Sharp *et al.* (1981) observed that earthquakes are related to flank eruptions in the area surrounding the volcano, with earthquakes preceding eruptions. However, Nercessian *et al.* (1991), found that earthquakes mainly occurred at the end of eruptive periods. Gresta *et al.* (1994) compared the
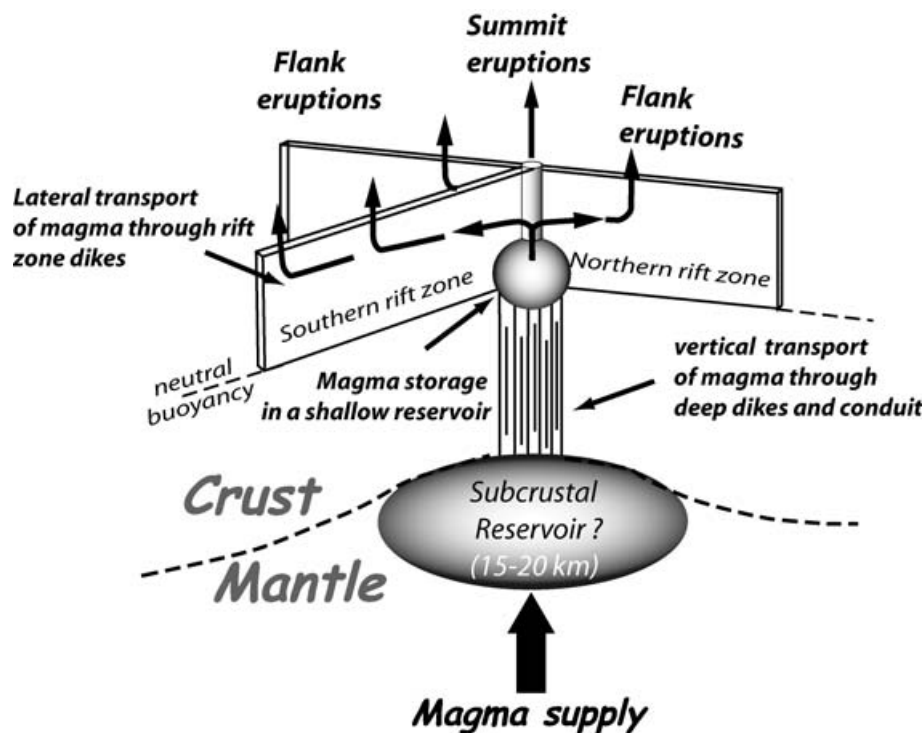

Figure 2. Simplified model of Mt Etna plumbing system. The subcrustal reservoir was inferred by Hirn *et al.* (1997) on the basis of seismological studies. These authors imaged the crust-mantle boundary at 15–20 km depth, beneath the eastern flank of the volcano, and suggested that the magma can be stocked in a lens capping the upper mantle at such depth. The presence of shallow reservoirs is inferred on the basis of seismological and geodetic data (see text). The southern rift zone is composed by two principal sets of dikes (∼N30°E and ∼ N160°E), whereas the northern rift zone is mainly composed of N30°E dikes. The magma can be driven in the lower crust through the central conduit system and deep dikes and further differentiated at shallow depth within the conduit itself, in a shallower plexus of dikes or in the superficial temporary small reservoirs before the eruptions (Condomines *et al.* 1995; Tanguy *et al.* 1997).
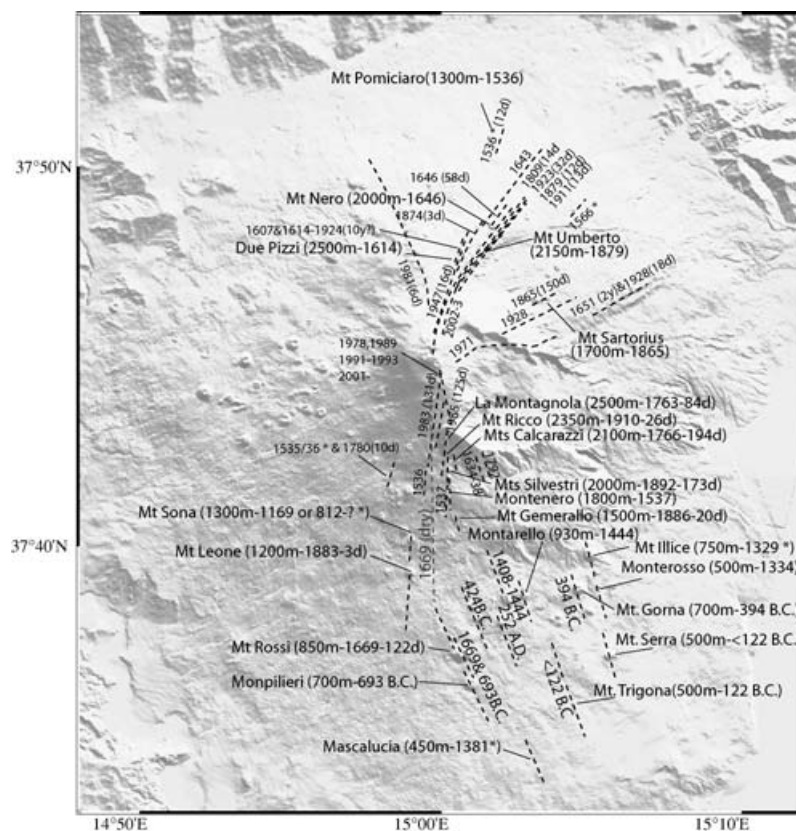
Figure 3. Main eruptive fissures associated with the rift zone eruptions since ∼700 B.C. Location of fissures retrieved using the descriptions of Romano & Sturiale (1982), Azzaro & Neri (1992) and the Mount Etna Geological Map (AA.VV 1979). Topography from the Digital Elevation Model (25 m of horizontal resolution) provided by the Istituto Nazionale di Geofisica e Vulcanologia, Catania, Italy. Dates with stars, probably older lava flows (see Tanguy *et al.* 1985, and Table 1).

timing of the largest eruptions (more than 10^7 m^3 of erupted products) with the largest earthquakes (I ≥ IX) that occurred within 30 km around the summit crater and found that earthquakes mainly occurred at the end of eruptive periods. Hirn *et al.* (1997) found that the occurrence of large ($M > 7$) sicilian earthquakes coincides with the end of episodes of high magma output rates.

To show a correlation between eruptions at Mt Etna and earthquakes close by, we examine the historical catalogue of Romano & Sturiale (1982) and Azzaro & Neri (1992) as well as the recent compilations by Acocella & Neri (2003) and Branca & Del Carlo (2004). We have discriminated flank eruptions, which are the most important in terms of erupted volumes, from the others. Since we mainly study the coupling between the rift zone dikes and the eastern Sicily normal faults, we report only the flank eruptions that occurred along the rift zone dikes (rift zone eruptions). Much less frequent flank eruptions occur along E–W-striking dikes, on the western flank or in the Valle Del Bove. Branca & Del Carlo (2004) have discussed the completeness of the eruptive catalogue at Mt Etna. It is complete since the 17th century for the largest eruptions. Its quality and completeness was greatly improved after the 1669 eruption and since the beginning of 19th century it contains no gap. The record of summit activity is continuous since the mid-18th century. The selected eruptions are summarized in Table 1.

On the basis of the information available in the historical catalogues and with the help of the 1/50 000 geological map (AA.VV 1979) we mapped the eruptive fissures for each eruption on the Etna digital elevation model (Fig. 3). The historical macroseis-

mic catalogue published by Azzaro *et al.* (2000, 2002) gives us a unique opportunity to compare the seismic activity on the Etna's eastern flank with the volcanic activity between 1855 and 2002.

In Fig. 4 we show the cumulative volumes erupted along the rift zone dikes (Table 1) since the 16th century, superimposed over the cumulative seismic moment released by the earthquakes that occurred in the eastern Sicily. This figure clearly shows the century-scale cyclic behaviour of Etna observed by Behncke & Neri (2003) with the highest volume erupted in the 17th century (episode R1). Three other periods of activity along the rift zone occurred between 1763 and 1809 (R2), between 1865 and 1928 (R3) and between 1971 and 1993 (R4, see Fig. 4). A further one initiated in 2001 with the eruptions of 2001 July–August, 2002 October to 2003 January and 2004 September to 2005 March. The cumulative seismic moment in eastern Sicily increases concurrently with erupted lava volumes. The 1693 January 11, the 1818 February 20 and the 1990 December 13 earthquakes occurred south of the volcano, at the end or few years after the end of a period of flank eruptions along the rift zone. The longer the period of rift zone activity, the larger the earthquake. The 1908 Messina and the 1783 Calabrian earthquakes occurred north of the volcano, farther from it, during an episode of rift zone activity (Fig. 4). A time correlation between rift zone eruptions and earthquakes might also exist for older periods. Palaeomagnetic data allowed dates of ancient lava flows to be better constrained (Tanguy *et al.* 1985; see Table 1 and Fig. 3) and revealed that other large rift zone eruptions with a significant effusion rate occurred during
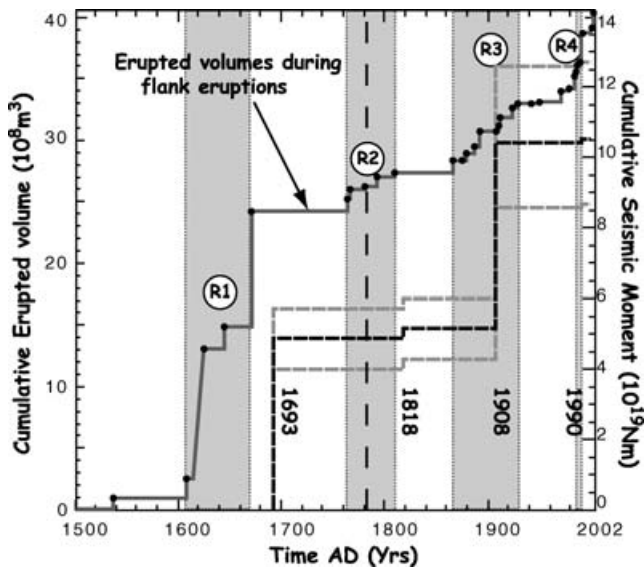
Figure 4. Cumulative volume of volcanic products erupted along the northern and southern rift zone dikes since the 16th century (see Table 1; Romano & Sturiale 1982; Acocella & Neri 2003; Branca & Del Carlo 2004) and the cumulative seismic moment released during the main earthquakes in eastern Sicily (1693 January 11, 1818 February 20, 1908 December 28 and 1990 December 13). The Calabrian earthquake of 1783 February 5 is also indicated by a vertical dashed line. In grey with numbers (R1–R4): periods of rift zone activity.

the 12th century before the 1169 earthquake (see also Hirn *et al.* 1997).

In Fig. 5(a) we show the location of small earthquakes ($M < 5$) that have produced macroseismic effects in the Etnean area between 1855 and 2002 (Azzaro *et al.* 2000, 2002). To compare the seismic activity of the faults on the Etna eastern flank and the eruptive activity during this period, we selected only the events located east of the volcano (dashed box in Fig. 5a).

Fig. 5(b) shows the variations of the annual rates of lava erupted along the rift zone compared to the variation of the annual seismicity rates on the Etna's eastern flank between 1855 and 2002. By calculating the sliding averages of both annual rates (seismicity and erupted lava) over 21 yr (we choose this time interval because it corresponds to the duration of periods of rift zone activity R3a, R3b and R4 shown in Fig. 6), we show a clear correlation between eruptive and seismic activities: the correlation coefficient *R* between the sliding averages of annual rates is equal to 0.87 (Fig. 5b, inset). The two main episodes of rift zone activity (1865–1928 and 1971–1993) are associated with two periods of strong seismic activity with several tens of $M \geq 3$ earthquakes per year.

In Fig. 6 we show the cumulative number of summit and rift zone eruptions (panels a and b, respectively) and the cumulative number of earthquakes (panels c and d). In Fig. 6b, we have also indicated the cumulative volumes of lava erupted along the rift zone and we show that the number of earthquakes increases simultaneously with the volume of lava and with the number of eruptions. This is particularly true for the largest magnitude earthquakes ($M \geq 3$) that occurred far from the rift zone, in the area of the 1818 main event, along the faults of San Leonardello, Moscarello, Trecastagni and Acireale (Fig. 6c, see fault locations in Figs 1b and 5a). Moreover, Fig. 6(a) shows that between 1928 and 1971, during a prolonged period of quiescence in the rift zone, the volcanic activity is quite intense at the summit of the volcano. In greater detail, between 1865 and 1928

(the time interval indicated by R3 in Fig. 4), there are two periods in which both the rift zone eruptions and seismic activity increased (R3a and R3b in Fig. 6). The large 1908 December 28 earthquake occurred at the beginning of the period named R3b; more precisely, 8 months after the first rift zone eruption occurred on 1908 April 29 (see Table 1).

Fig. 6(c) shows that the seismic activity decreased after 1993, at the end of the huge 1991–1993 rift zone eruption, whereas it begins to increase since 2001 in concomitance with the latest rift zone eruptions of 2001 and 2002–2003. Recent data recorded between 2002 June and 2003 February have shown a sharp increase of the seismic activity along faults located on the eastern flank of the volcano 2 weeks after the beginning of the 2002 northern rift zone eruption (Acocella *et al.* 2003). During this period, more than 20 earthquakes with magnitude ranging between 3.5 and 4.4 occurred along the Pernicana and the Acireale–Piedimonte fault systems (Azzaro *et al.* 2003); some of them caused macroseismic effects and damages.

Fig. 7 shows the temporal sequence of eruptions separated into rift zone eruptions, other flank eruptions (which occurred along the western and eastern flanks) and summit eruptions and compares them with the largest magnitude earthquakes, which struck eastern Sicily. As previously discussed, the 1693 earthquake occurred after the large flank eruptions of the 17th century (indicated by R1 in Fig. 4). Fig. 7 reveals that after the 1693 event, no rift zone eruptions were reported during the following 70 yr. However, the volcanic activity at the beginning of the 18th century (after the 1693 earthquake) was concentrated in the summit crater. Another period of rift zone inactivity occurred after the 1818 earthquake, but it was slightly shorter (56 yr) than that which followed the 1693 seismic event.

Figs 6(a) and 7(c) suggest that during the quiescent periods along the rift zone the summit eruptions are quite frequent. This is evident for the period 1723–1759, named S1 in Fig. 7(c). However, during the periods labelled S2 and S4 in Fig. 7 the volcanic activity interested both the summit and the rift zone areas.

All these observations suggest that a two-way mechanical coupling (that is a mutual interaction) exists between eruptions at Etna volcano and earthquakes that struck eastern Sicily. These observations and findings have motivated the numerical modelling of earthquake-volcano interaction through elastic stress transfer that we will discuss in the following.

5 MODELLING ELASTIC STRESS TRANSFER

We aim to investigate the interaction between earthquakes and volcanic eruptions by modelling the static stress changes caused by dislocations. Elastic stress perturbations caused by earthquakes are represented by changes in volumetric or normal stress near the magma chamber, conduits or eruptive dikes, while stress changes caused by volcanic sources are represented by Coulomb stress perturbations on assumed fault planes (e.g. Savage & Clark 1982; Nostro *et al.* 1998; Toda *et al.* 2002). We performed all calculations in a homogeneous Poissonian elastic half-space using the FARFALLE code (Nostro *et al.* 2002), limiting our investigations to the instantaneous elastic effects. We set the Lamé's constants equal to 32 Gpa.

We first calculate the changes in Coulomb stress caused by volcanic eruptions at Mt Etna on the neighbouring fault planes that ruptured during the large Sicilian earthquakes. Given the uncertainties on the storage zones, we consider several geometries for reservoirs

Table 1. Etna rift zone eruptions from the historical catalogue of Romano & Sturiale (1982) and the update compilation of Acocella & Neri (2003) and Branca & Del Carlo (2004). All historical references are cited in these two papers. SA: Summit activity, SRZ: southern rift zone, NERZ: Northeastern rift zone, F: formation, CC: central crater, NEC: Northeastern crater, VDB: Valle Del Bove, E.F: Eastern flank.

Date	Location	Duration (days)	Lava vol. (10^6 m^3)	Fissures orientation	Altitude a.s.l. (m)	Comments
693 B.C.	SRZ	—	—	NNW–SSE?	650	F. Monpilieri?
425 B.C.	SRZ	—	—	NNW–SSE?	900	F. Mt Arso?
394 B.C.	SRZ	—	—	NNW–SSE?	700	F. Mt Gorna
122 B.C	SRZ – SA[a]	—	—	NNW–SSE?	450	F. Mt Trigona
<122 B.C.	SRZ	—	—	NNW–SSE?	550	Cones located at Trecastagni
<122 B.C.	SRZ	—	—	NNW–SSE?	450	F. Mt Serra
252–253 A.D.	SRZ	—	—	NNW–SSE?	850 -760	F. Mt Peloso
970 – 1200 [a]	NE Flank	—	—	ENE–WSW	975 m (lava)	F. Mt Rinatu (980 ± 60 BP)
812 or 1169[e,c]	SRZ	—	—	N–S?	1200	South Mt Sona
1329 –28 Jun[c]	SRZ	—	187	NNW–SSE?	725	Fissure crosses Mt Illice
1334	SRZ	—	60	NNW–SSE?	500	F. Monterosso
1381 August 5[b]	SRZ	—	76	NNW–SSE	450–350	Near Mascalucia, F. Mts. Arsi St. Maria and Cicirello
1408 November 9[d]	SRZ	12	—	NNW–SSE	950 (1200[a])	North of Mt Arso (5 vents near Monte Albero)
1444	SRZ	20?	—	NNW–SSE	950 (1200[a])	North Mt Arso, F. Montarello, collapse of C.C. at end
1535 or 1536[c]	SRZ	—	—	NNE–SSW	2000	F. Mt Nero degli Zappini
1536 March 22[c]	SRZ -NERZ	12	90 (only NERZ)	NNE–SSW	1900–1400	F. Mt Pomiciaro. Strong seismic activity on the southern flank
1537 May 11	SRZ	18	—	NNE–SSW	1800–1500	F. Mt Nero and Palombaro. Collapse of C.C. at end
1566 November[b]	NERZ	—	40	NNE–SSW	1400	—
1607- 28 Jun	SRZ	—	165	ENE–WSW	2250–1950	Strong earthquakes
1614 -1 Jul → 1624	NERZ	3650?	1050	NNE–SSW?	2550	F. Mt Deserti –Due Pizzi- strong explosion at CC
1634 December 19 → 1638	SRZ	850?	—	NNW–SSE	2100–1950	near Mt Serra Pizzuta Calvarina
1643 February	NERZ	—	—	NNE–SSW	2100–1275	—
1646 November 20 → 1647	NERZ	58	180	NE–SW	2000–1800	F. Mt Nero and Ponte di Ferro
1669 March 11	SRZ	122	937	NS to NNW–SSE	850–800	N–S fracture between the summit to Nicolosi (dry)-Collapse C.C at end Very strong and destructive earthquakes before the eruption
1763 – 18 June	SRZ	84	100	NNE–SSW	2500	F. La Montagnola
1766 April 27	SRZ	194	75	N–S	2100–1950	F. Mts Calcarazzi –Violent earthquakes on southern flank
1780 May 18	SRZ	10	28	NNE–SSW?	2350–1850	Explosive activity at C.C. before
1792 May 26 → 1793	SRZ	380?	80	NNW–SSE	~2000	Explosive activity at C.C. before
1809 March 27	NERZ	14	36	NNE–SSW	CC to 1300	Began at the summit
1865 January 30	NERZ	150	96	ENE–WSW	1825 - 1625	7 eruptive cone. F Mts Sartorius
1874 August 29	NERZ	2	1.3	NNE–SSW	2450–2200	—
1879 May 26	NERZ	12	50	NNE–SSW?	2400?-1690	also on SW Flank- F. Mt Umberto and Margherita
1883 March 22	SRZ	3	0.05	NNE–SSW	1200–950	F. Monte Leone – 8 eruptive cones
1886 May 19	SRZ	20	66	NNW–SSE	1500–1300	F. Mt Gemmellaro. explosion at C.C. before
1892 July 9	SRZ	173	120	NNE–SSW & NS	2025–1800	F. Mt Silvestri
1908 April 29	SRZ	1	1.2 (*2*)	NNW–SSE	2500–2275	7 eruptive cones – explosive activity at CC before
1910 March 23	SRZ	26	44 (*65*)	NNE–SSW	2350–1950	F. Mts Ricco – 15 eruptive boccas

Table 1. (*Continued.*)

Date	Location	Duration (days)	Lava vol. (10^6 m^3)	Fissures orientation	Altitude a.s.l. (m)	Comments
1911 September 10	NERZ	13	63 (*55*)	NE–SW	2250–1650	—
1918 November 30?	NERZ- SRZ		*1.22*	NNW–SSE & NS	2850–3050	explosive activity at CC before
1923 June 17	NERZ	31	78	NE–SW	2500–1800	—
1928 November 2 —	NERZ	18	42 (*40*)	ENE–WSW	2600–1200	Destruction Mascali
1942 June 30	SRZ	1	1.6	NNE–SSW	2800–2400	12 explosive boccas
1947 February 24	NERZ	16	10 (*11.8*)	NNE–SSW	NEC-2200	explosive activity at NEC before
1949 December 5	NERZ	3	6 (*10*)	NNW–SSE	Summit-2000	
1971 April 5	SRZ -EF	69	75 (*11.7*)	WNW–ESE	3050–1800	F. Mts Ponte
1975 February 24	NRZ	187	6	NNW–SSE	2625	—
1975 November 29	NRZ	406	*29.4*	NW–SE & NNW–SSE	2980–2900	F. Mt Cumin
1978 April 29	SRZ	37	27.5	NNW–SSE	3000–2000	—
1979 August 3	NERZ	6	7.5	ENE–WSW & WNW–ESE	2950–1700	
1981 March 17	NRZ	6	30	NNW–SSE	2550–1140	—
1983 March 28	SRZ	131	100	NS	2680–2250	—
1985 March 12	SRZ	125	30	NNE–SSW	2620–2480	—
1986 October 30	NRZ	122	57 (*60*)	E–W	3350–2180	—
1989 September 27	SRZ-NRZ-VDB	10	26 (*38.4*)	NNW–SSE & ENE–WSW	2950–1510	Flank fracture: dry. Eruptive between 2950–3000 m
1991 December 14	SRZ	473	231 ± 29	NW (3.4 Km)	3100–2400	—
2001 July 17	VDB-SRZ-	23	48 (*25.2*)	N–S NNE N–S	3020–2980 2850–2650 21 90–2060	—
2002 October 27	NERZ	8	10	NE	2500–1900	—
2002 October 27	SRZ-	93	74.5	NNW–SSE	2850–2600	—

[a]see Branca & Del Carlo (2004).

[b]Lava flow dated by palaeomagnetism at 1050–1250 AD (Tanguy *et al.* 1985).

[c]Lava flow dated by palaeomagnetism at 700 and 1000 AD (Tanguy *et al.* 1985).

For the 1536, only the northern lave flows are older. For 1329 one lava flow at Mt Illice is older.

[d]Lava flow located at Trecastagni and inferred to be erupted in 1408 could be prehistoric (Tanguy *et al.* 1985).

[e]The date of this eruption is doubtful since its corresponds also with the large 1169 Sicilian earthquake (Romano & Sturiale 1982).

Volume in italic from Acocella & Neri (2003).

such as spherical, sill shaped or dike shaped. Voiding/filling of the magma reservoir is represented by closing/opening the walls of vertical dikes or horizontal sills or by deflation/inflation of a spherical cavity. The spherical reservoir is approximated using three orthogonal dikes, which is equivalent to a Mogi (1958) point source if the volume change is scaled by a factor *b* (see e.g. Nostro *et al.* 1998; Feigl *et al.* 2000; Feuillet *et al.* 2004). For the dike- shaped reservoir, we used two different orientations, E–W and N–S.

The Coulomb stress changes are calculated using the widely adopted relation (e.g. Harris 1998; King & Cocco 2000):

$$\Delta \text{CFF} = \Delta\tau + \mu(\Delta\sigma_n + \Delta P), \tag{1}$$

where $\Delta\tau$ is the shear stress change computed in the direction of slip on the secondary fault, $\Delta\sigma_n$ is the normal stress changes (positive for extension), μ is the coefficient of friction and ΔP is the pore pressure change. For simplicity, we considered here a constant effective friction model (see Beeler *et al.* 2000; Cocco & Rice 2002), which assumes that ΔP is proportional to the normal stress changes ($\Delta P = -B\Delta\sigma_n$, where *B* is the Skempton parameter). According to this assumption, Coulomb stress changes are calculated through the relation:

$$\Delta \text{CFF} = \Delta\tau + \mu'\Delta\sigma_n, \tag{2}$$

where μ' is the effective friction [$\mu' = \mu(1 - B)$]. The fault is brought closer to failure when ΔCFF is positive. We used a value of 0.5 for μ', which is equivalent to laboratory value of friction and modest fluid pressure (e.g. Nostro *et al.* 1998). Several authors

(Nostro *et al.* 1998; King & Cocco 2000, among others) have shown that the Coulomb stress changes are modestly sensitive to the μ' value.

In order to model the stress transferred by large magnitude earthquakes onto the Etna plumbing system, we calculated the horizontal normal stress changes caused by planar dislocations on the rift zone dikes (or on dike-shaped reservoirs) as well as the pressure changes ($\Delta P = \Delta\sigma_{kk}/3$, negative for compression) on spherical reservoirs. For the sill-shaped reservoir, we calculated the vertical stress change ($\Delta\sigma_{zz}$). To evaluate the effect of an earthquake on the Etna vertical conduit, we calculated the horizontal stress changes around a cylinder ($\Delta\sigma_{xx} + \Delta\sigma_{yy})/2$.

The calculation of elastic stress changes requires the knowledge of the geometry of tectonic and volcanic sources. We will briefly describe this issue in the following of this section, while the results of numerical calculations will be presented in the next section.

5.1 Earthquake source models

The calculation of static stress changes caused by shear dislocations requires selecting the earthquake source parameters: fault dimensions, orientations, faulting mechanism and slip amplitude. The source parameters adopted in this study are listed in Table 2. Two fault models have been proposed for the 1693 earthquake: we first assume that it occurred offshore along a main normal fault that follows the Malta escarpment (hereinafter called solution 1).
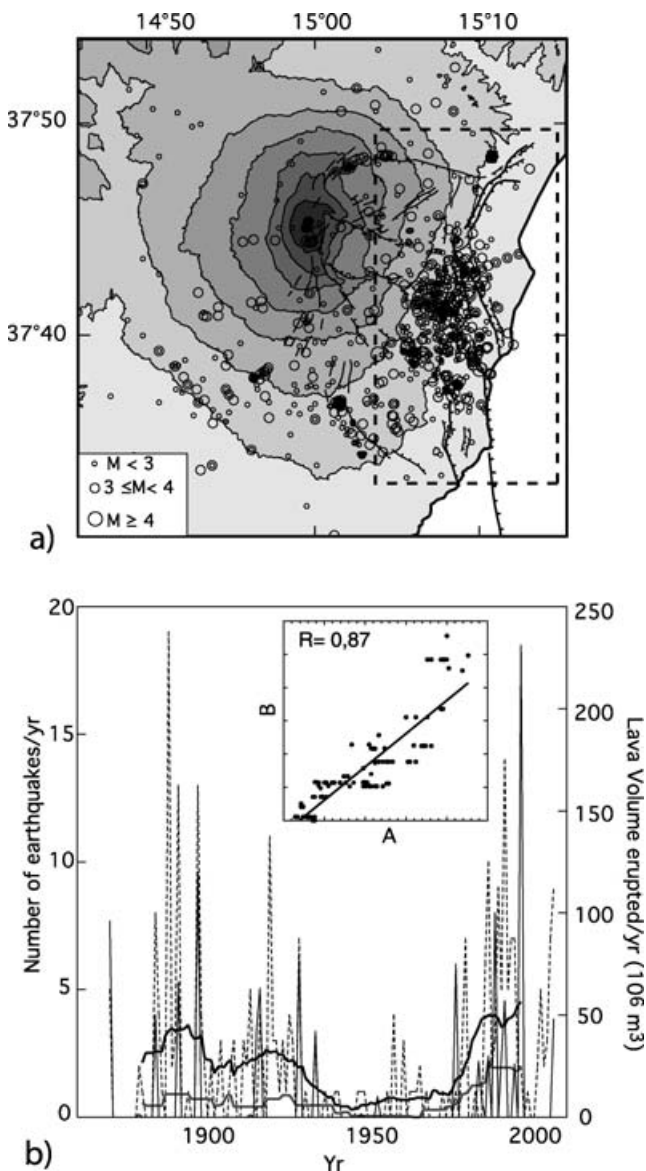
Figure 5. (a) Epicentres of earthquakes, which have produced macroseismic effects in the Etnean area between 1855 and 2001 from Azzaro *et al.* (2000), Azzaro *et al.* (2002). Dashed box: earthquakes that produced macroseismic effect on the eastern flank along the Acireale–Piedimonte faults, selected for the plots of Figs 5(b), 6(c) and (d). (b) Thin dashed line: annual rates of $M \geq 3$ earthquakes, which produced macroseismic effects in the Etnean area and the sliding averages over 21 yr (thick black line). Thin black line: annual rates of lava (10^6 m^3 yr^{-1}) erupted along the rift zone and, the sliding averages over 21 yr (thick grey line). Inset: 21-yr sliding averages of annual seismicity rates (A) as a function of 21-yr sliding averages of annual rates of lava erupted along the rift zone (B). A and B correlate linearly with a coefficient *R* equal to 0.87.

Based on geological, morphological and offshore data, Bianca *et al.* (1999) proposed the following source model for this event: it occurred along a 45-km-long, NNW–SSE-striking, east-dipping normal fault segment having a right-lateral component of motion. We assume the width of the ruptured fault segment to be 20 km, in agreement with both the magnitude (>7.0) of the 1693 event and the thickness of the seismogenic crust (e.g. Jacques *et al.* 2001). We also calculated the stress changes induced by a shallower rupture (10 km of width). We suggest that this event may have ruptured F4

or F3 fault mapped by Hirn *et al.* (1997) and shown on Fig. 1(a). An alternative source model (hereinafter called solution 2) has been proposed for the 1693 earthquake by Sirovich & Pettenati (1999). Solution 2 is adopted by the DISS (Database of Italy's Seismogenic Sources, e.g. Valensise & Pantosti (2001). Following Sirovich & Pettenati (1999), this earthquake ruptured an 80-km-long, N12°E-striking, N80° eastward-dipping dextral strike-slip blind fault segment in the Hyblean plateau. However, there are several problems with this model. No fault with clear morphologic evidence of activity can be associated to this fault plane; it is difficult to reconcile this source model with the tsunami observed during the 1693 earthquake (Piatanesi & Tinti 1998) and the faulting mechanism is not compatible with the present-day regional stress field in this part of Sicily (NNW compression, see Musumeci *et al.* 2005). Nevertheless, we have used this fault model to compute the stress changes on the Etna plumbing system, adopting a more realistic rupture length of 45 km. We also test the case of a sinistral component of motion, which is more consistent with the inferred regional stress field (Musumeci *et al.* 2005).

Several source models have been proposed for the 1908 Messina strait earthquake, based on the analysis of geodetic or seismological data (see e.g. Pino *et al.* 2000, and references therein). We adopted the model proposed by Boschi *et al.* (1989) since it is in agreement with the geology and the long-term morphology of the Messina strait, with the historical levelling data and with the waveforms recorded at regional distances (Valensise & Pantosti 1992; Pino *et al.* 2000). This model consists of a single fault 45 km long and 18 km wide, dipping 30° eastward and striking N11.5°E with pure normal faulting mechanism. For the 1783 earthquake sequence (February 5, 6, 7 and March 1) we use the source model proposed by Jacques *et al.* (2001), which is based on a seismotectonic study combined with the analysis of damage patterns. The 1783 sequence ruptured several N50° ± 20°E-striking, west-dipping normal fault segments. The February 5 main event ruptured three different segments for a total length of 45 km and a moment magnitude larger than 7. The subsequent events were smaller ($M = 6, 6.5$) and ruptured a fault segment near Scilla (on February 6) and two normal fault segments north of the February 5 ruptures (on February 7 and March 1). The seismic moment estimated for the first February 5 shock is close to $7 \cdot 10^{19}$ N m (Jacques *et al.* 2001).

The 1818 February 20 earthquake ($M \sim 6$, intensity up to IX-X, Boschi & Guidoboni 2001) occurred on the eastern flank of Mt Etna, north of Catania, along the Acireale fault (see Fig. 1b and Azzaro & Barbano 2000). It probably ruptured the entire 10 km long fault. The fault plane geometry was determined by microtectonics measurements (Monaco *et al.* 1997). To calculate the static stress changes caused by this event, we considered a square fault with a length of 10 km reaching the surface and dipping 60° eastward. We assumed a slip direction equal to that of the slickensides observed on the fault plane (rake = 40°; Monaco *et al.* 1997). The rupture dimension that we adopted is in agreement with that proposed by Barbano & Rigano (2001) on the basis of macroseismic data. According to the Wells & Coppersmith (1994) empirical relation, a 10-km-long and 10-km-wide rupture would produce an earthquake of moment magnitude equal to 6.3, in agreement with Boschi & Guidoboni (2001). The scaling relationship proposed by Kanamori (1977) yields a slip of ∼1 m.

5.2 Volcanic source models

The periods of rift zone activity with large erupted volumes of lava contribute to empty the temporary reservoirs where magma was
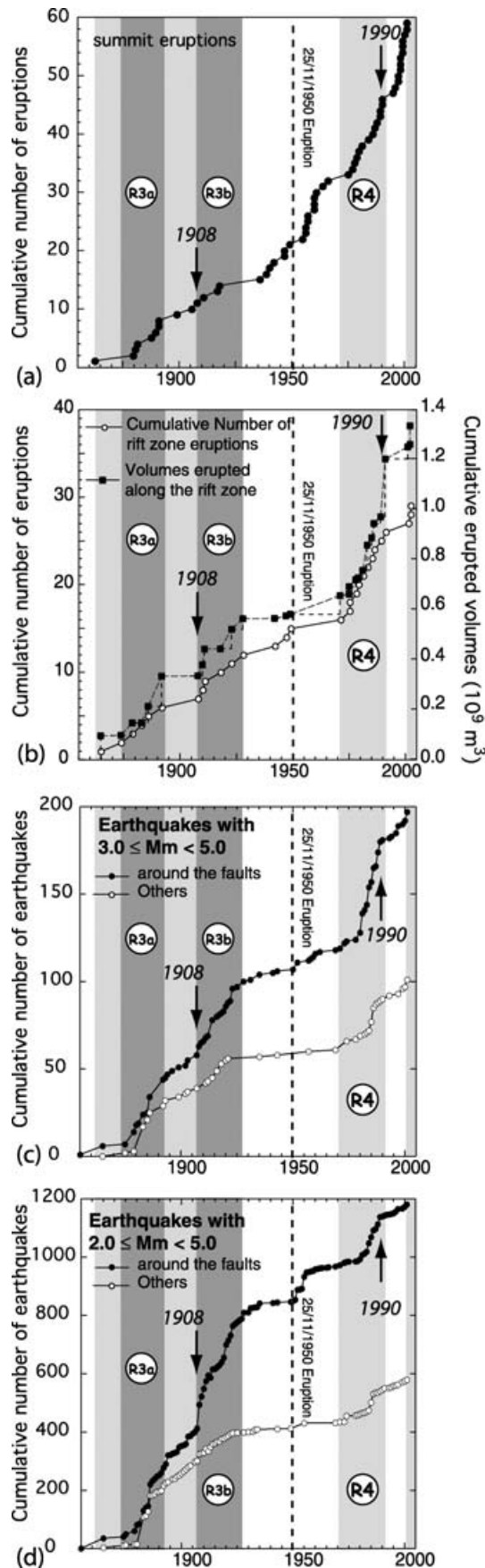
previously accumulated. For example, the geodetic measurements performed at Mt Etna between 1980 and 1993 (Bonaccorso 2001) revealed that the volcano inflated during the 10 yr preceding the 1991–1993 eruption. Most of the deformation was subsequently released during the eruption, which was conversely associated with a strong areal contraction of the volcano. The ground deformation pattern has been interpreted as the joint effects of the depressurization of a shallow reservoir due to magma output and a tensile dislocation corresponding to the uprising of the magma through feeder fractures (Bonaccorso 1996). To examine the effect of Etna rift zone eruptions on the eastern Sicily normal faults, we thus calculated the Coulomb stress changes caused by the opening of the rift zone dikes and the voiding of shallow reservoirs. All modelling parameters are listed in Table 3 and described below.

According to fluid-mechanical models for magma transport in dikes (e.g. Lister & Kerr 1991), the volcanic rift zone probably developed around and in connection with the storage zone. This allows the magma to migrate laterally, at the level of neutral buoyancy, far from the summit area. We propose that the rift zone dikes extend from the storage zone (reservoir, conduit or plexus of dikes) to the Earth's surface (Fig. 2). The principal limitation of our calculations is the lack of information on the depth of the feeder dikes and reservoirs of the past flank eruptions. Recent geophysical and seismological studies suggest that magma may be stored in small reservoirs between 3 and 6 km below sea level (Bonaccorso 1996; Puglisi *et al.* 2001; Lundgren *et al.* 2003; Patanè *et al.* 2003; Bonaccorso *et al.* 2004). According to these results we adopt an average depth of 5 km for the reservoirs. This value is in agreement with the level of neutral buoyancy at Mt Etna (Corsaro & Pompilio 1998). The dikes of the rift zone are connected with the reservoir and reach the surface, having a total width of 5 km. These values agree with the results of Bonaccorso *et al.* (2002) and Aloisi *et al.* (2003) who determined widths ranging between ∼2.0 and ∼4.5 km for the eruptive dikes of the 2001 and 2002–2003 flank eruptions.

Magma storage at greater depth (between 9 and 16 km) has been also inferred by analysing InSar data (Massonnet *et al.* 1995; Delacourt *et al.* 1998; Lanari *et al.* 1998). We will also consider in our simulations volcanic source models with deeper reservoirs

Figure 6. (a) Cumulative number of summit eruptions since 1855 (data from Branca & Del Carlo 2004). All eruptions at the summit are reported except the Strombolian activity. (b) Cumulative number of rift zone eruptions since 1855 and cumulative erupted volumes along the rift zone (10^6 m^3). Data from Romano & Sturiale (1982), Azzaro & Neri (1992), Acocella & Neri (2003) and Branca & Del Carlo (2004). (c) and (d) Cumulative number of earthquakes that produced macroseismic effects in the Etnean area between 1855 and 2001. Databases from Azzaro & Barbano (2000), Azzaro *et al.* (2002). (c) Earthquakes with magnitude ranging between 3.0 and 4.9 and (d) with magnitude ranging between 2.2 and 4.9. Black circles: cumulative number of earthquakes located on the eastern flank of Mt Etna close by or along the Acireale–Piedimonte fault system, with epicentres within the dashed box of Fig. 5a. White circles: other earthquakes of the Etnean area. The large earthquakes that occurred in the eastern Sicily are indicated with arrows. In grey: episodes of rift zone activity. Episode R3a, between 1874 and 1892, episode R3b, between 1908 and 1928. We indicated by a dashed line the huge flank eruption of 1950 November 25 to 1951 December 2 (171×10^6 m^3 of erupted lava) that occurred on the eastern flank of Mt Etna along an E–W-striking fissure in the Valle Del Bove. This eruption was followed by numerous small earthquakes occurred on the eastern flank of the volcano (Fig. 6d).
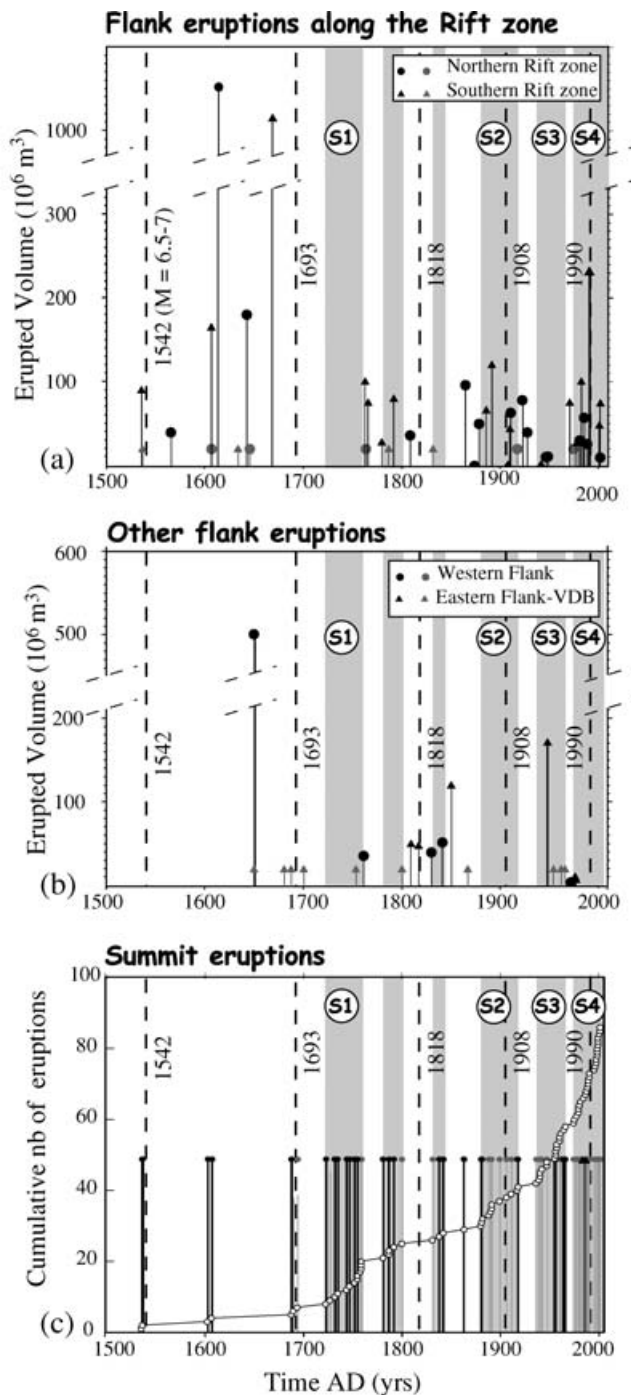
Figure 7. Eruptions chronology versus erupted volume. Data from Romano & Sturiale (1982), Azzaro & Neri (1992), Acocella & Neri (2003) and Branca & Del Carlo (2004). (a) Flank eruptions along the rift zone dikes. In grey: eruptions without information on the erupted volumes. (b) Eruptions along other dikes on the western or eastern flanks. Colours as in (a). (c) Summit area eruptions. In black with circles: main submittal eruptions between 1500 and 1974 from Romano & Sturiale (1982). In grey with circles and in black with triangles: all submittal eruptions (Central and NE and SE craters, Bocca Nuova) between 1500 and 2002 from Branca & Del Carlo (2004). For all eruptions represented with circles (black or grey), we have no information on the volumes of lava erupted. White circles: cumulative number of eruptions at the summit. The main eastern Sicily earthquakes are indicated with dashed lines.

(10 and 15 km) and wider rift zone dikes. Our results and interpretations do not change significantly, except for the earthquakes located on the eastern flank of Mt Etna (i.e. the 1818 event), as we will discuss in the next sections.

We calculate the cumulative Coulomb stress changes caused by repeated eruptions along the rift zone dikes as a single process represented by the expansion (dilation) of the entire rift zone. In this way we avoid need in to specify the details of the geometry and the opening of each single dike associated with each eruption. We believe that this is accurate enough for the purposes of this study. We provide different models for each period of rift zone activity as a function of the number of eruptions along the northern or the southern rift zones and the length of the dikes. The opening of the rift zone dikes during the eruptions of the last twenty years was inferred from geodetic data modelling (Bonaccorso 1996, 2001; Bonaccorso *et al.* 2002; Aloisi *et al.* 2003). It ranges between 1 and ~5 m, with an average value of 2.3 m. To model the rift zone total dilation, we multiply this average opening by the number of eruptions occurred along the southern or the northern rift zones. We have large uncertainties on the opening of the rift zone dikes. However, since the elastic Coulomb stress changes increase linearly with the volumetric changes, this parameter does not affect the Coulomb stress change pattern (see e.g. Nostro *et al.* 1998).

We modelled the rift zone expansion associated with the large 17th-century flank eruptions preceding the 1693 earthquake by using two dikes striking N165°E and N30°E for the southern and northern parts, respectively. The northern rift zone dike is 12 km long whereas the southern one is 20 km long, in agreement with the length of the eruptive fissure opened during 1669 eruption (see Fig. 3). Six eruptions occurred during this period, three along the southern rift zone and three along the northern one. We have fixed the total opening of both rift zones to 7 m. We modelled the eruptions that occurred at the end of the 18th century along the southern rift zone by using a 6.5-km-long dike, oriented N–S (average strike of eruptive dikes during this period, see Fig. 3) and opened by ~9 m (four eruptions). Only one eruption occurred before the 1818 earthquake along the northern rift zone, in 1809. The fissure associated with this eruption is about 7.5 km long and strikes N30°E. We set the opening of the dike to 2.3 m. In order to evaluate the influence of the dike orientations, we also calculate the stress changes induced by the 1792 eruption on the 1818 fault rupture (see Table 3 for dike parameters). This eruption occurred closer to the fault, along a N160°E-striking dike (see location on Fig. 3). To model the Coulomb stress changes caused by the rift zone eruptions of the end of the 19th century (phase R3a) on the 1908 earthquake, we used two dikes with lengths of 7.5 and 12 km for the northern and the southern rift zones, respectively. Each dike is opened by 7 m.

The change in volume of the reservoirs depends on the erupted volume of lava during each period we considered. As an example, during the 17th century about 2400×10^6 m^3 of lava erupted along the rift zone. For this period, we set a total volumetric decrease of about 2400×10^6 m^3 in the reservoirs.

We also calculate the Coulomb stress increase induced by the reservoir refilling after the rift zone eruptions. Such periods are likely associated with summit eruptions (Meriaux & Jaupart 1995). During the eruptions at the summit, the central conduit probably dilates. We calculate the Coulomb stress changes induced by the expansion of a cylindrical conduit above the reservoirs. We considered here an open conduit and simulated it by the opening of two vertical orthogonal dikes.

Table 2. Earthquake parameters.

Date	I_{max}	M_e	M_w	M_o N m	L km	W km	Strike deg	Dip deg	Rake deg
1693 January 11[1]	XI[a]	7.1		$4 \times 10^{19(e)}$ $5.7 \times 10^{19(f)}$	45	20	340.0	60	−120.0
1693 January 11[2]	XI[a]	7.1			45	20	10.0	80	(−130.0) 40.0
1783 February 5[b]	XI		7.0	7×10^{19}	10 30 6	20 20 20	250.0 220.0 200.0	70 60 65	−75 90 −95
1783 February 6[b]	IX		6.3	3.7×10^{18}	14	14	245.0	65	−75
1783 February 7[b]			6.5	6.2×10^{18}	17	17	220.0	65	90
1783 March 1[b]			5.7	3.9×10^{17}	7	7	200.0	65	−95
1818 February 20[d]	X	6.2		$2.5 \times 10^{18(f)}$ $3.2 \times 10^{18(g)}$	10	10	350.0	60	−130
1908 December 28[c]	XI		7.1	$5.4 \pm 2 \times 10^{19}$	45	18	11.5	29	90°

[a]Boschi & Guidoboni (2001).
[b]Solution from Jacques *et al.* (2001).
[c]Solution from Boschi *et al.* (1989).
[d]Solution from this study and Azzaro *et al.* (1991).
[e]Boschi *et al.* (1995).
[f] Azzaro & Barbano (2000).
[g]This study.
[1] Solution 1: Bianca *et al.* (1999).
[2] Solution 2: Sirovich & Pettenati (1999) and rake modified in agreement with the regional stress of the Hyblean plateau (Musumeci *et al.* 2005).

Table 3. Volcanic sources parameters.

Eruption Dates	Type		Lat. °N	Lon. °E	Depth km	Dip deg	Strike deg	L km	W km	Slip m
1607–1614–1634	Rift zone	Northern dike	15.026	37.797	0.0	90.0	30.0	12.0	5.0	7.0
1643–1646–1669		Southern dike	15.017	37.665	0.0	90.0	160.0	20.0	5.0	7.0
1763–1766–1780	Rift zone	Northern dike[a]	15.016	37.783	0.0	90.0	30.0	7.4	5.0	9.0
1792–1809		Southern dike	14.991	37.721	0.0	90.0	180.0	6.5	5.0	2.3
1792	Rift zone	Southern dike	15.008	37.721	0.0	90.0	160.0	6.5	5.0	2.3
1865–1874–1879	Rift zone	Northern dike	15.016	37.783	0.0	90.0	30.0	7.4	5.0	7.0
1883–1886–1892		Southern dike	14.996	37.683	0.0	90.0	0.0	12.0	5.0	7.0
All eruptions	Spherical reservoir voiding/ filling*		15.000	37.750	5.0	—	—	—	—	—
All eruptions	Sill-shaped reservoir voiding/filling*		15.000	37.750	5.0	0.	0.	5.0	5.0	
All eruptions	N–S dike-shaped reservoir voiding/filling*		15.000	37.750	5.0	90.0	0.0	10	10	
All eruptions and eastern and western flanks	E–W dike-reservoir voiding/filling* or E–W striking feeder dikes closing/opening		15.000	37.750	5.0	90.0	90.0	10	10	
All summits	Conduit expansion		15.000	37.750	0.0	90.0	—		10[b]	—

[a]only 1809 (see Table 1).
[b]conduit length.
*volumetric changes are function of erupted volumes during each period of flank activity.

5.3 Modelling uncertainties

The most evident limitation in modelling stress interaction between earthquakes and volcanoes is the lack of precise information on the location and geometry of the volcanic and seismic sources for past earthquakes and eruptions (see also Nostro *et al.* 1998). Nevertheless, the available information on earthquakes and volcanic eruptions in this area allows us to constrain simple source models, which are accurate enough to discuss the spatial pattern of elastic stress perturbations. However, there are two important limits in our study: first, we only analyse static stress changes and neglect other time-dependent processes, such as viscoelastic relaxation, which may modify the stress change pattern (e.g. Hill *et al.* 2002, and references therein); second, we cannot take into account the real topography in our modelling approach (we calculate the stress changes in a flat half-space). The computation of elastic stress changes including the real topography of the volcano is beyond the goals of the present study.

We consider here a homogeneous elastic half-space with $\lambda = \mu$, implying a Vp/Vs ratio equal to 1.73 and a Poisson's ratio of 0.25.

However, the velocity models calculated by Laigle *et al.* (2000) reveal small wavelength anomalies of the Vp/Vs ratio ranging between 1.64 and 1.90, beneath the volcano. This would imply a variation of the Poisson's ratio of ± 20 per cent compared with our Poisson solid approximation. Laigle *et al.* (2000) and Chiarabba *et al.* (2000) show the presence of a high Vp body (with P-wave velocity ranging between 5.5 and 7 km s^{-1}) extending between 2 and 18 km depth beneath Mt Etna. Given these velocity values, the density of rocks beneath the Etnean area (Corsaro & Pompilio 2003) and the Poisson solid approximation, one would determine values of shear modulus ranging between 26 and 48 GPa within the crust beneath the volcano. These variations of elastic modulus may alter the stress change pattern. In our calculations we use a value of 32 Gpa. At the base of the crust, where the shear modulus is higher, the stress change values would increase by about 50 per cent. Near the surface, where the shear modulus is lower than 32 Gpa, the stress change values would conversely decrease by nearly 20 per cent compared with our results.

6 NUMERICAL RESULTS

The results of our numerical calculations are summarized in Tables 4 and 5 and are shown in Figs 8–12. We first show and discuss the Coulomb stress changes caused by either rift zone eruptions or magmatic inflation of the storage zones on the faults that ruptured during large historical earthquakes (Table 4, Figs 8 and 9). Afterwards, we present the stress perturbations generated by earthquake dislocations on the Etna volcano (Table 5, Figs 10–12).

6.1 Eruptions promoting earthquakes

Figs 8(a) and (b) show the Coulomb stress changes caused by the 17th-century rift zone eruptions on the faults planes that are believed to have ruptured during the 1169 and 1693 $M > 7$ earthquakes. Fig. 8(a) shows the effects of the rift zone dilation, whereas Fig. 8(b) shows the combined effects of the rift zone dilation and the voiding of a shallow reservoir. Fig. 8(c) shows the Coulomb stress changes caused by the rift zone eruptions at the end of 19th century (rift expansion only) on the fault plane, which ruptured during the 1908 Messina earthquake. In all cases, the Coulomb stress increased in lobes located at the tips of the rift zone and beneath it. All large earthquakes occurred where the Coulomb stress increased. The 17th-century rift zone eruptions increased the Coulomb stress by more than 0.1 MPa on a large portion of the F3 and F4 normal faults and may have triggered the 1693 earthquake, which occurred 25 yr after the last eruption. The flank eruptions that occurred at the end of the 19th century, before the 1908 Messina earthquake, increased the Coulomb stress on the causative fault by less than 0.1 MPa (Fig. 8c). The pattern of the Coulomb stress changes is modified by adding the effect of the reservoir voiding (Fig. 8b), which tends to slightly decrease the Coulomb stress along the fault planes that ruptured in 1693 and 1908 (see Table 4). We have calculated that both the inflation of a magmatic reservoir (spherical or sill shaped) and the expansion of a cylindrical conduit, which are likely associated with volcanic activity at the summit, increased slightly the Coulomb stress on both fault planes (see Table 4).

Modelling elastic stress transfer caused by volcanic eruptions on the 1693 earthquake and assuming that its causative fault is located inland in the Hyblean plateau (solution 2, adopting either a left- or a right-lateral strike-slip mechanism) yields very small stress perturbations and, therefore, the interaction is weak: the rift zone

Table 4. Coulomb stress interaction between volcanic sources and earthquakes.

	1693/01/11 F4 and F3	1818/02/20	1908/12/28
Rift zone expansion	+ +	− − −[a]	+
Spherical source Deflation	−	+ + +	−
Spherical source Inflation	+	− − −	+
Sill Deflation	−	See Fig. 9	−
Sill Inflation	+	See Fig. 9	+
NS dike-shaped reservoir deflation	− −	+ + +	−
NS dike-shaped reservoir inflation	+ +	− − −	+
EW dikes (feeders or reservoir) deflation	+ +	+ + +	+
EW dikes (feeders or reservoir) inflation	− −	− − −	−
Conduit expansion	+	− −	+

[a] + for 1792 eruption

where:

(+ or −) corresponds to Coulomb stress changes of $\pm$ 0.1 MPa at most.

(++ or − −) corresponds to Coulomb stress changes of $\pm$ 0.5 MPa at most.

(+++ or − − −) corresponds to Coulomb stress changes larger than ± 0.5 MPa.

dilation produces positive but small (less than 0.05 MPa) Coulomb stress changes along the fault (Table 5). The stress changes caused by Mt Etna eruptions on the 1783 Calabrian earthquake are negligible. This may suggest that this event, distant from the volcano, does not interact with volcanic sources.

Fig. 9 shows the Coulomb stress changes transferred either by the voiding of reservoirs (of various shapes and depths) or by the rift zone expansion on the fault plane which ruptured during the 1818 February 20 earthquake. Coulomb stress changes are calculated on the basis of the volumes of lava erupted between 1763 and 1809, before the 1818 earthquake (see Table 3). However, we used the same modelling results to interpret the timing and distribution of the smaller earthquakes that occurred in the Etnean area. First, because the pattern of the elastic Coulomb stress changes is independent of the volumetric changes. Second, because we considered that all these earthquakes ruptured fault planes identical to that ruptured in 1818. In Fig. 9 we reported the epicentres of the earthquakes that produced macroseismic effects in the Etnean area between 1855 and 2002. Only the most recent earthquakes, for which hypocentral depths were computed (Azzaro *et al.* 2002), are reported on vertical cross-sections. The events, which occurred on the eastern flank of the volcano, close by or along the Acireale–Piedimonte fault system (plotted in white on Fig. 9), have depths ranging between 0 and 10 km.

The voiding of a shallow (5 km) spherical reservoir during the rift zone eruptions increases strongly the Coulomb stress along the Acireale–Piedimonte fault system (by more than 1 MPa by making the calculations with the volumes erupted between 1763 and 1809) and may have promoted the 1818 February 20 earthquake as well as the smaller ones on the eastern flank of the volcano (Fig. 9a). The distribution of the earthquakes coincides well with the pattern of Coulomb stress increase; most of the events are located in an area of enhanced Coulomb stress. The result does not change if the spherical reservoir is deeper (15 km, Fig. 9e); the increase in Coulomb stress is however smaller.

The voiding or filling of a sill-shaped reservoir may produce large stress changes on Mt Etna eastern flank faults. The results differ as

Table 5. Stress interactions between earthquakes and the plumbing system calculated along a vertical profile located beneath the summit of the volcano (15.00°E, 37.75°N).

	N30°E dike (normal stress)	N160°E dike (normal stress)	EW dike (normal stress)	Spherical source (pressure)	Sill (normal stress)
1693/01/11 solution 1 on F4, $W = 20$ km	$- -^a$	$+$	$- -$	$-$	$+^b$
1693/01/11 solution 1 on F4, $W = 10$ km	$- -^c$	$+$		$-$	
1693/01/11 solution 1 on F3, $W = 20$ km	$- -^d$	$++$		$-$	
1693/01/11 solution 1 on F3, $W = 10$ km	$- -^e$	$++$		$- -^c$	
1693/01/11 solution 2 right-lateral motion	$+$	$-$		$-$	
1693/01/11 solution 2 left lateral motion	$-$	$+$		$+$	
1783 February–March	$+$	$+$	$+$	$-$	$-$
1818/02/20	$- -^e$	$-^f$	$- -$	$-$	$-^h$
1908/12/28	$+$	$-$	$-$	$-$	$+^g$

Where:

($+$ or $-$) corresponds to normal stress or pressure changes of ± 0.1 MPa at most.

($++$ or $- -$) corresponds to normal stress or pressure changes of ± 0.5 MPa at most.

($+++$ or $- - -$) corresponds to normal stress or pressure changes larger than ± 0.5 MPa.

Normal stress changes are positive for extension. Pressure changes are negative for compression.

W: Width.

[a]($+$) for depth larger than 35 km.
[b]($-$) for depth larger than 10 km.
[c]($+$) for depth larger than 25 km.
[d]($+$) for depth larger than 30 km.
[e]($+$) for depth larger than 20 km.
[f]($+$) for depth larger than 15 km.
[g]($-$) for depth larger than 27 km.
[h]Larger values for depths ranging between 10 and 20 km.

a function of the reservoir depth. The voiding of a shallow (5 km) sill-shaped reservoir decreases the Coulomb stress on a large portion of the fault plane, except near the surface (Fig. 9b). However, when the reservoir is deeper (15 km), the Coulomb stress increases on the whole fault plane (Fig. 9d).

Tensile dislocations induce a strong Coulomb stress decrease on both sides of the rift zone (Fig. 9c). By using the volumes erupted between 1763 and 1809, we calculated that the Coulomb stress decreased by more than 1 MPa along the fault plane ruptured in 1818. However, the Coulomb stress increases around the dike tips, where numerous damaging earthquakes occurred during the rift zone eruptions, particularly on the southern flank of the volcano, around the town of Nicolosi (Fig. 9c). We calculated that the expansion of the central conduit decreases the Coulomb stress along the Mt Etna eastern flank faults (Table 4).

6.2 Earthquakes effects on eruptions

Figs 10 and 11 show the normal stress and pressure changes caused by the eastern Sicily earthquakes (1693, 1818 and 1908), as well as by the 1783 Calabrian event on the Etna plumbing system. The results are also summarized in Table 5. For simplicity, we prefer to show the elastic stress changes induced by each earthquake along a vertical profile located beneath the summit of the volcano instead of displaying maps. The normal stress and pressure changes are positive for extension. Fig. 11 illustrates the stress changes generated by different fault models adopted for the 1693 earthquake (solution 1, considering a rupture either on fault F3 or F4 with a width of 10 and 20 km; solution 2, either with a right- or a left-lateral compo-

nent of motion). Our modelling results show that the 1783 and the 1908 earthquakes caused small stress perturbations in comparison with the earthquakes that occurred south of the volcano (Fig. 10). The stress changes induced by the 1693 event are very small if we consider that it occurred in the Hyblean plateau (solution 2, see Fig. 11). In the following, we focus our discussion on the stress changes caused by the 1693 (solution 1) and the 1818 earthquakes.

6.2.1 Effects on dikes

Our calculations show that the 1818 earthquake, located very close to Mt Etna, caused the largest stress changes on the volcano, despite its smaller magnitude. This event produced a horizontal normal stress gradient (up to 0.2 MPa) along the N0° $\pm$ 30°E-striking dikes, with a small extension at depth, switching to compression towards the surface (Figs 10a, b and f). The shallower the rupture, the shallower the depth at which the extension switches to compression (see Fig. 11a and Table 5). Such a gradient can favour the opening and propagation of the dikes at depth and their closing towards the surface. The 1693 earthquake induced a comparable horizontal stress gradient along the N30°E-striking dikes and unclamped the N160°E-striking ones at all depths (Fig. 11b). Both earthquakes induced a compression, which increases towards the surface, on the E–W-striking dikes (Fig. 10e). The stress changes caused by the 1693 earthquake depend on the location of the fault and on the adopted source parameters (Fig. 11). A shallow rupture (less than 10 km wide) along the F3 fault (Hirn *et al.* 1997, see Fig. 1a), closer to the volcano than F4, can generate the greatest effects on the rift zone, comparable with that produced by the 1818 event. Such a
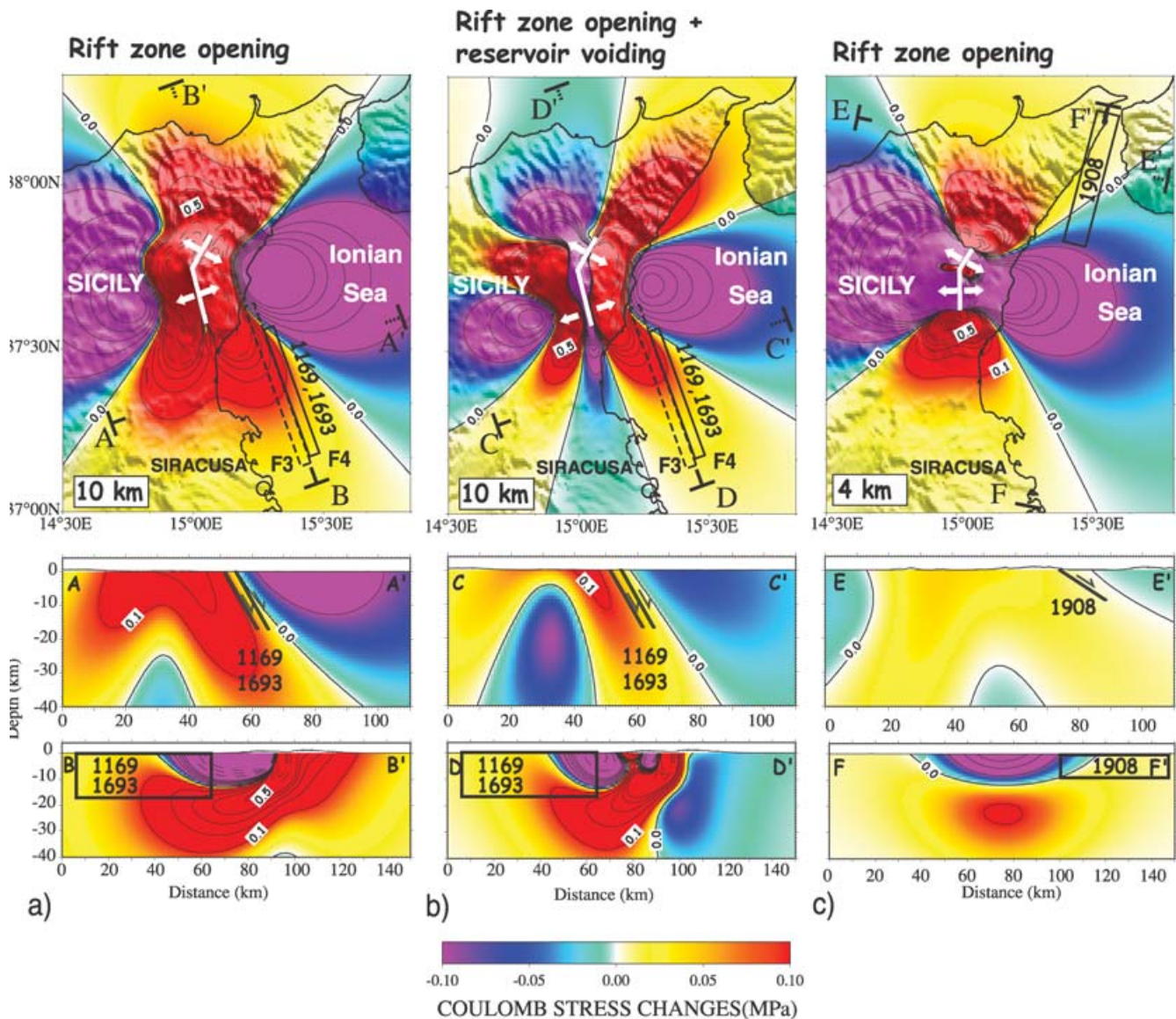
Figure 8. Coulomb stress changes, calculated at ∼mid-depth of the seismic faulting (10 km for the 1169 and 1693 earthquakes and 4 km for the 1908 one) and in vertical cross-sections, with topography (bottom panels, topography as in Fig. 3) due to: (a) a dilation of 7 m of the rift zone between 0 and 5 km of depth associated with the 17th-century eruptions (see Table 3 for parameters) on a 160°N-striking right-lateral (rake = −120°) normal fault with a dip of 60° towards east (1693 earthquake, solution 1). (b) As in (a) but the rift zone dilation is associated with the reservoir voiding at 5 km depth with a volumetric loss of 2400 × 10^6 m^3. (c) a dilation of 7 m of the rift zone between 0 and 5 km of depth associated with the end of the 19th-century eruptions (see Table 3 for parameters) on a N11.5°E-striking normal fault with a dip of 29° towards east (1908 earthquake fault rupture after Boschi *et al.* 1989). For all calculations, the apparent coefficient of friction is 0.5. Contours: each 0.1 MPa (continuous lines) between −0.5 and 0.5 MPa, each 0.5 MPa (dashed lines) between −2 and 2 MPa. Ruptured planes indicated by boxes.

rupture compresses the N30°E- striking dikes by more than 0.3 MPa. In Fig. 12 we show the normal stress changes caused by the 1693 earthquake (solution 1 on fault F4 with a width of 20 km) on the rift zone dikes as a function of their strikes. This earthquake tends to compress all the N30°E-striking dikes of the rift zone with stronger normal stress to the south (more than 0.2 MPa, Fig. 12a). It also compresses the N–S-striking dikes that are located mainly near the summit (Fig. 12b), whereas it creates an extension on the N160°E-striking dikes (Fig. 12c), with the exception of those located south of Nicolosi, where the dikes are strongly clamped by the earthquake (Fig. 12c). It is interesting to note that, since the 1693 earthquake, no eruption occurred on the N160°E-striking dikes south of Nicolosi (Fig. 3).

6.2.2 Effect on reservoirs

The 1818 earthquake may have contributed to compress crustal magmatic reservoirs of different geometries by decreasing the pressure around a spherical cavity (Fig. 10c) and the normal stress on the walls of dike-shaped (striking both E–W and N–S, Figs 10e and f, respectively) or sill-shaped reservoirs (Fig. 10d). For the spherical or dike-shaped reservoirs, the coupling is much more efficient near the surface. The 1818 earthquake has decreased the vertical stress beneath Etna, with the largest values at a depth of 15 km (Fig. 10d). This would have compressed by ∼0.03 MPa a sill-shaped subcrustal reservoir (lens), such as that inferred by Hirn *et al.* (1997) (see Fig. 2). The coupling between the other earthquakes and the sill-shaped reservoir seems to be less relevant.
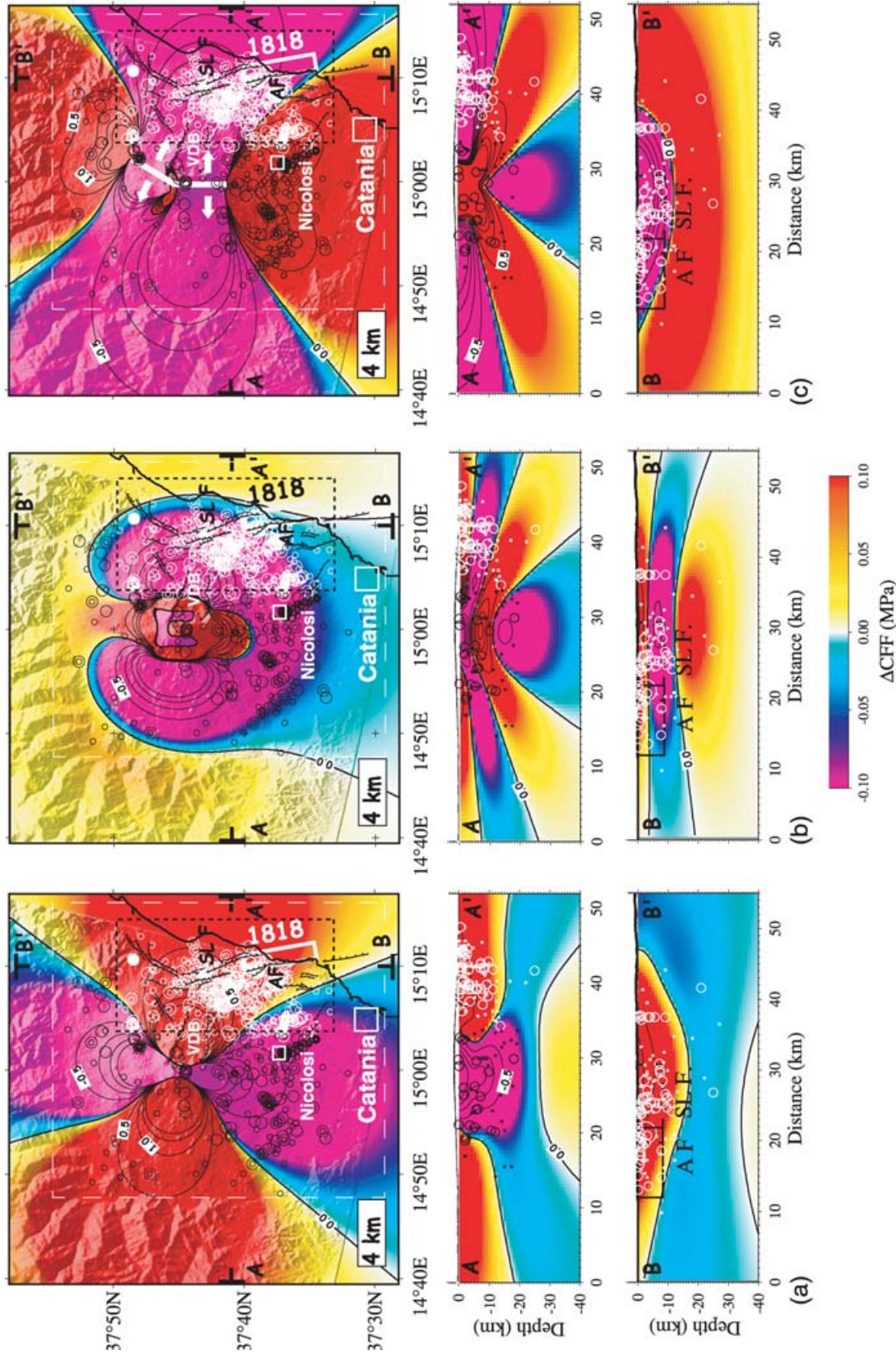
Figure 9. Coulomb stress changes in map at 4 km depth (about the half-width of the 1818 rupture) and in W–E and S–N cross-sections with topography (bottom panel, topography as in Fig. 3) induced on a 170°N-striking right-lateral (rake = −130°) normal fault with a dip of 60° towards east by (a) the voiding of a spherical magmatic reservoir at 5 km depth (the volumetric loss corresponds to the lava volumes erupted before the 1818 earthquake (375 × 10⁶ m³); (b) the collapse (voiding) of a sill-shaped reservoir located at 5km depth (volumetric loss as in Fig. 9a); (c) the opening of the rift zone dikes between 0 and 5 km of depth associated with the eruptions which occurred between 1763 and 1809 before the 1818 earthquakes (see Table 3 for parameters); (d) the collapse of a sill-shaped reservoir located at 15km depth (volumetric loss as in Fig. 9b) and (e) the voiding of a spherical magmatic reservoir at 15 km depth (volumetric loss as in Fig. 9a). The epicentres of earthquakes, which produced macroseismic effects on Etnean area, are reported in white for the earthquakes located close by or along the Acireale–Piedimonte fault system (earthquakes located in the dashed black box) and in black for the others. Databases from *Azzaro et al.* (2000), *Azzaro et al.* (2002). The dashed white box indicates the geographical boundaries of the data set. Only the most recent earthquakes, whose hypocentral depths are known, are reported in cross-sections. Apparent coefficient of friction as in Fig. 8. Contours each 0.5 MPa between −2 and 2 MPa. The 1818 rupture plane indicated in the white box.
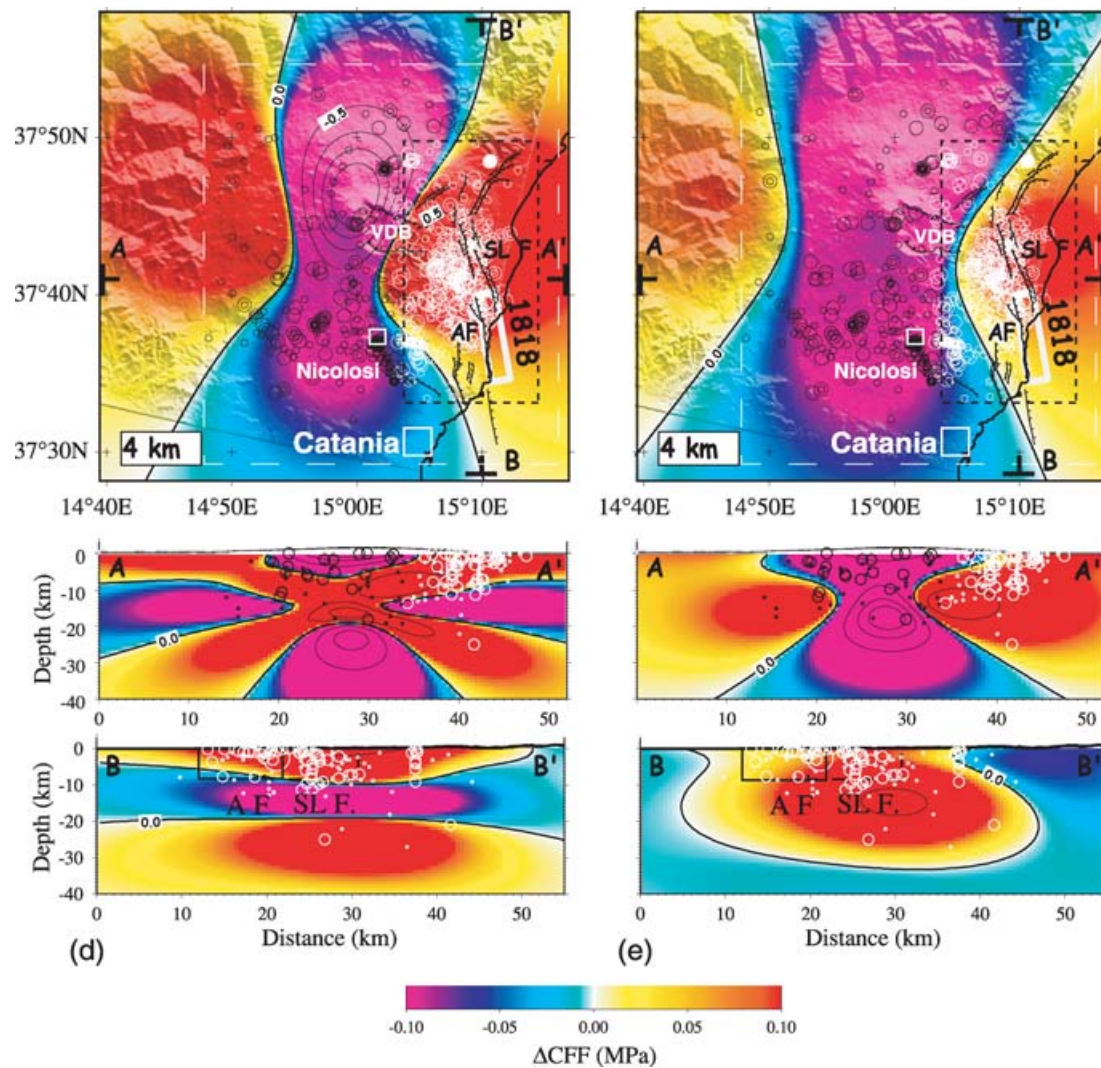
Figure 9. (*Continued.*)

The 1693 earthquake has also compressed a spherical reservoir as well as an E–W-striking dike-shaped reservoir (Figs 10c and e). The coupling is more efficient for a shallow rupture on the F3 fault with a pressure decrease up to 0.1 MPa (Fig. 11c). The 1693 event can slightly unclamp a N–S-striking dike-shaped reservoir (Fig. 10f).

7 DISCUSSION

In this study, we examined the mechanical coupling between Mt Etna's eruptions and a large normal fault system active along the eastern coast of Sicily. This fault system is responsible both for large historical earthquakes ($M > 6$) in Sicily and for numerous smaller ones on the eastern flank of Mt Etna. To do that, we calculated the static Coulomb stress transferred by the eruptions to the fault planes and the pressure or normal stress changes produced by an earthquake around the volcano.

Modelling the Coulomb stress changes induced by the volcanic activity at Mt Etna helps us to understand the distribution and timing of damaging earthquakes around the volcano. We showed that eruptions along the rift zones are able to increase by several tens of MPa the Coulomb stress on the eastern Sicily normal fault planes and may have promoted both the large historical earthquakes and

the numerous smaller ones on the eastern flank of the volcano. The rift zone eruptions are likely associated with the opening and propagation of feeder fractures and the voiding of shallow reservoirs. The earthquakes located on the eastern flank of the volcano, as the 1818 one, are promoted by the voiding of the reservoirs, whereas the 1693 and 1908, located further south and north of the volcano, at the tips of the rift zone, are promoted by the opening of feeder fractures. In the same manner, the earthquakes responsible for macroseismic effects on the eastern and western flanks of the volcano were likely promoted by the voiding of the reservoirs while the tensile dislocations along the rift zones promoted those on the northern and southern flanks.

In Fig. 4 we showed that the larger earthquakes occurred at the end or few years after a period of rift zone eruptions. The larger the volumes of lava erupted, the larger the earthquake. We also showed that the seismic activity around the volcano, and particularly along the eastern flank faults, increases concurrently with the cumulative lava volumes erupted along the rift zone dikes (Figs 6b and c). The larger the volumes erupted, the higher the seismic activity along the faults. This may be explained by the fact that the Coulomb stress increases as the volume (pressure) of the reservoirs decreases and as the feeder fractures open. Several studies
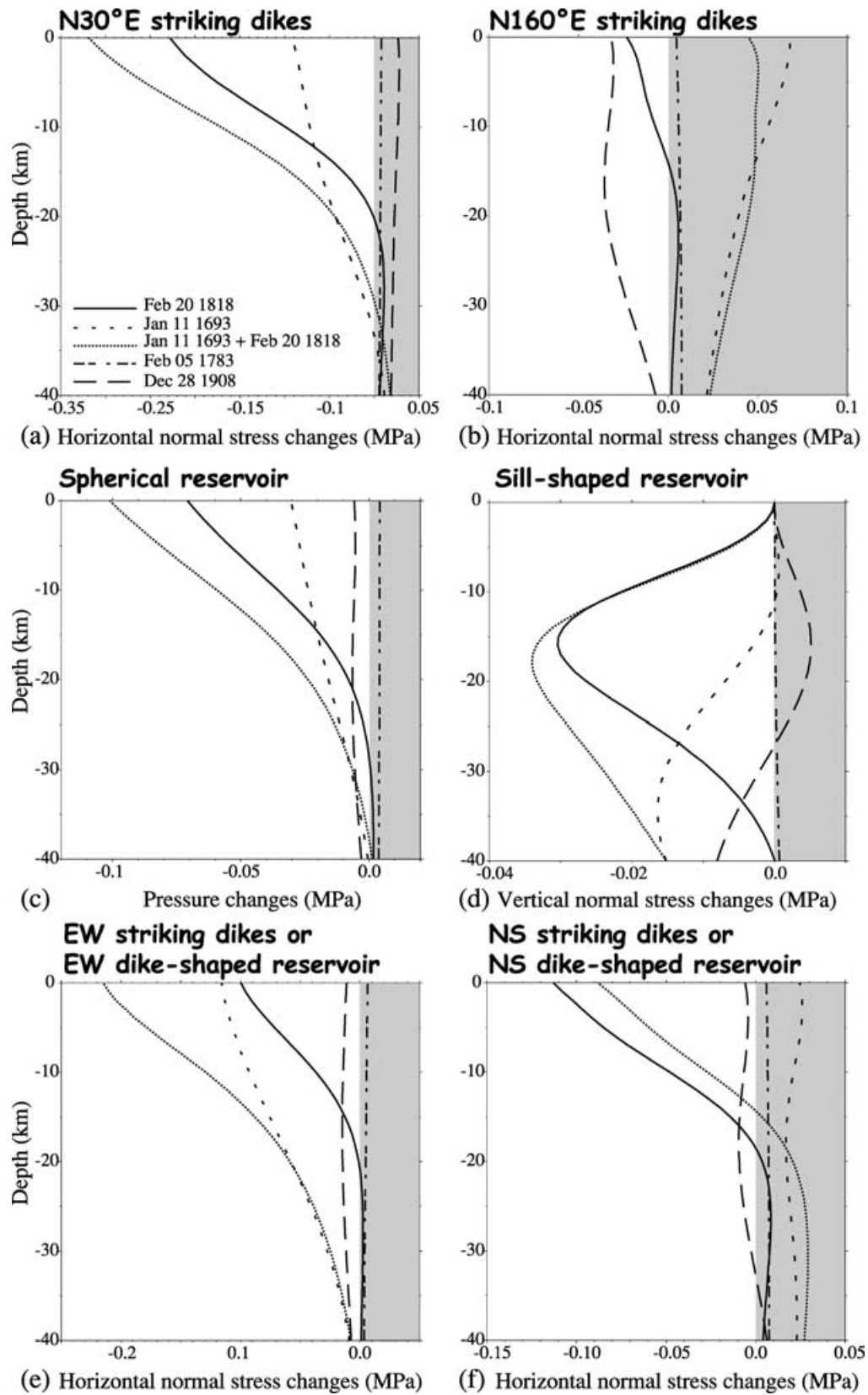
Figure 10. Normal stress and pressure changes induced by the eastern Sicilian earthquakes beneath the summit of the volcano (15.00°E, 37.75°N). (a) Normal stress changes on vertical N30°E-striking dikes; (b) normal stress changes on vertical N160°E-striking dikes; (c) pressure changes; (d) vertical stress changes; (e) normal stress changes on vertical E–W-striking dikes and (f) normal stress changes on vertical N–S-striking dikes. In grey: zone of tensile stress. In Fig. 10(c), the white zone corresponds to a compression of a spherical reservoir.

N30°E striking dikes

(a)   Normal stress changes (MPa)

N160°E striking dikes

(b)   Normal stress changes (MPa)

Spherical reservoir

(c)   Pressure changes (MPa)
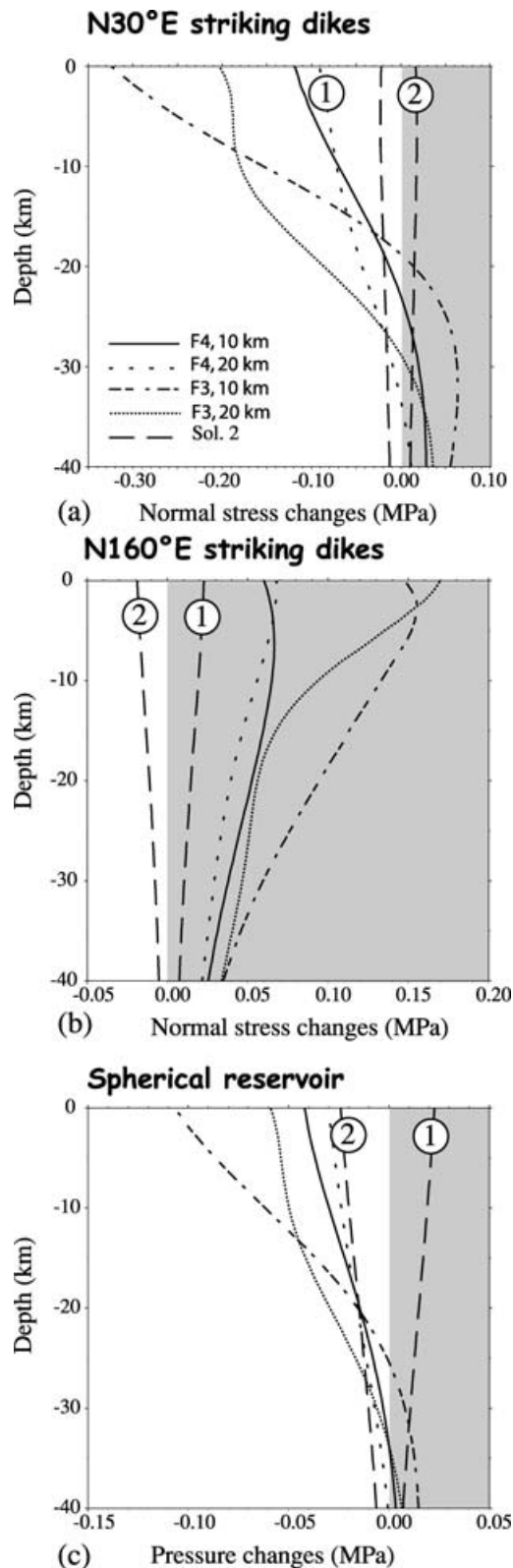
Figure 11. Normal stress and pressure changes induced by the 1693 earthquake beneath the summit of the volcano (15.00°E, 37.75°N), considering several source parameters for the earthquake (see text and Table 2). Number 1: 1693 earthquake, solution 2 with left lateral motion; number 2: 1693 earthquake, solution 2 with a right-lateral motion. a) normal stress changes on vertical N30°E-striking dikes; b) horizontal normal stress changes on N160°E-striking dikes; c) pressure changes.

have shown that the seismicity rate depends on the Coulomb stress changes (Stein 1999, and reference therein, Dieterich *et al.* 2000; Toda *et al.* 2002). This dependence can be modelled by using the rate/state constitutive law of Dieterich (1994), which relates the rate of earthquake occurrence to the stressing rate. For example, Toda *et al.* (2002) show that the change in seismicity rates during the 2000 eruption of Izu in Japan was proportional to the stressing rate induced by the opening of a propagating dike. One may thus infer that the larger the lava volumes erupted at Mt Etna, the larger the strain and stress around the volcano and the larger the seismicity rate. We speculate that the largest earthquakes (1169, 1693, 1818 and 1990) occurred when the Coulomb stress was high along the fault system, at the end of the eruptive activity along the rift zone.

We showed that when the reservoirs recharge, the Coulomb stress strongly decreases along the eastern flank faults (this is however not true for a shallow sill-shaped reservoir). This may explain why the seismicity rate drops between periods of activity along the rift zone. The expansion of the central conduit could also contribute to the decrease of the seismic activity. We, however, showed that this two processes (reservoir refilling and conduit expansion) increased slightly the Coulomb stress along the faults that ruptured in 1693 (1169), according to solution 1, and in 1908 and may have also contribute to promote these large earthquakes.

The evolution of the seismic activity associated with the 2002–2003 rift zone eruption was described by Acocella & Neri (2003) and can be interpreted in terms of Coulomb stress transferred by the volcanic processes to faults. These authors showed that during the northwards propagation of the eruptive dike along the northern rift zone on 2002 October 26 and 27, the seismicity was concentrated only along the dike and propagated downrift with the dike. After the dike propagation, the eruption continued for 3 months and the earthquakes mainly occurred at the northern tip of the dike and on the eastern flank of Mt Etna, along the Pernicana and Acireale–Piedimonte faults. Such evolution of the seismicity agrees well with our modelling results. We showed that the opening of the dike induced a strong decrease of Coulomb stress on its both sides (Fig 9c), preventing the occurrence of earthquakes along the dike after its propagation. However, the Coulomb stress is increased around the dike tips promoting earthquakes. During the eruption, the reservoirs are progressively emptied generating an increase of Coulomb stress on the eastern flank along the Acireale–Piedimonte faults (Fig. 9a), where seismicity clustered between the 2002 October 26 and the end of the eruption (2003 January 28).

The static stress perturbations caused by earthquakes on the Etna plumbing system are of the order of 0.1 MPa and are small if compared to tectonic stresses, lithostatic pressures and magmatic chamber overpressures. They are, however, two orders of magnitude higher than the stress changes induced by ocean tides for which time correlation with volcanic activity has been observed in several cases (e.g. Kasahara 2002). Several studies based on physical models have shown that stresses induced by the load of a volcanic edifice (e.g. Watanabe *et al.* 2002; Pinel & Jaupart 2004) may affect the magma transport in dikes and its storage, if sufficiently strong (several MPa). These studies, however, faced the problem of magma migration through the crust on large timescales (several thousand years) and are based on simplified models. The Etna plumbing system is probably much more complicated and it is possible that small stress changes at the scales of few decades may affect the volcano activity. Among several others, Pinel & Jaupart (2004) have shown that the magmatic overpressure gradients in dikes control the storage or the lateral/vertical propagation of the magma beneath the
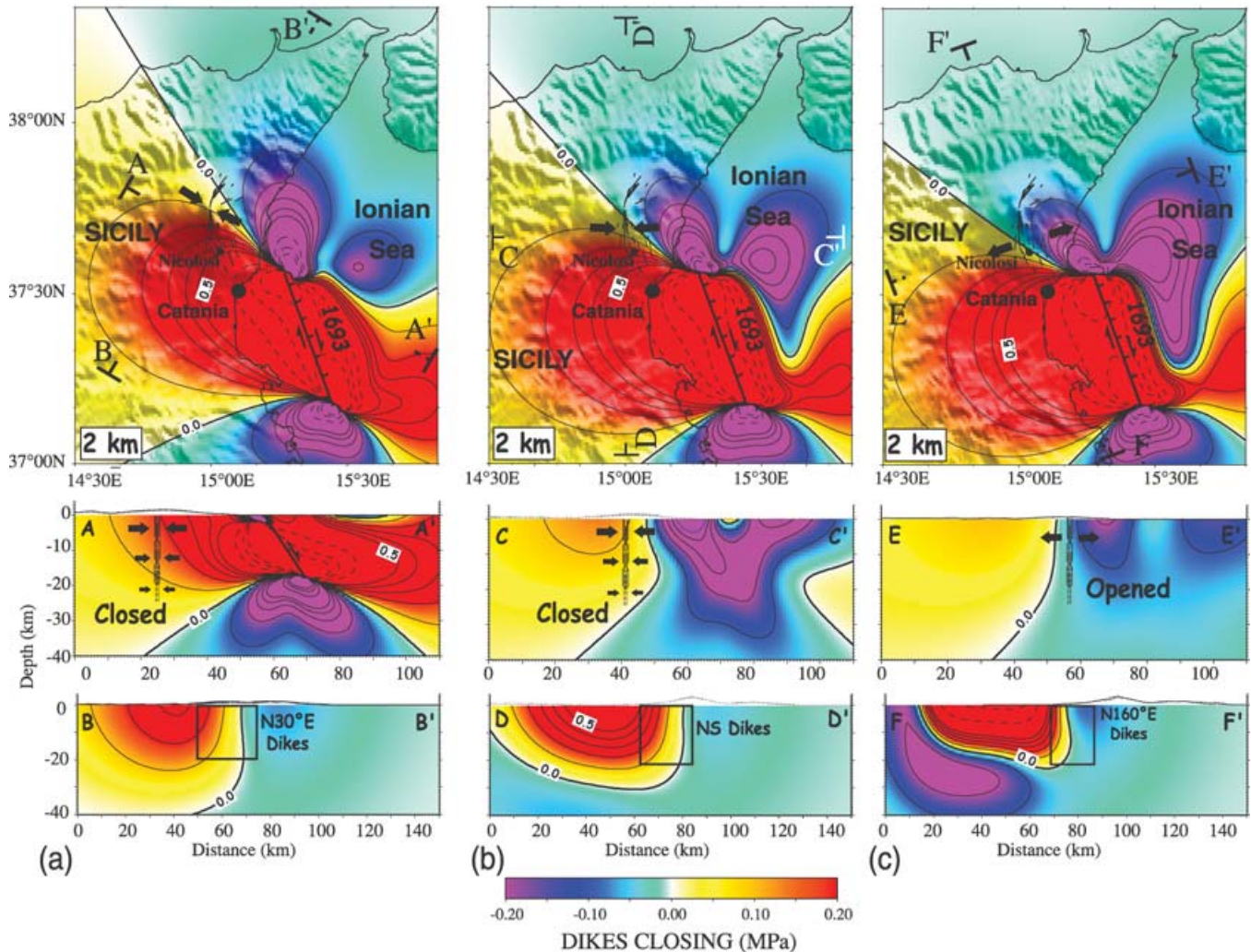
Figure 12. Normal stress changes in maps at 2 km depth and along cross-sections with topography (bottom panel, topography as in Fig. 3) induced by the $M > 7$, 1693 January 11 earthquake on (a) N30°E dikes; (b) N–S dikes; (c) N160°E dikes. Contours as in Fig. 8.

volcanoes. These overpressure gradients depend on several parameters, such as the magma buoyancy, the initial overpressure in reservoirs and the tectonic stress (e.g. Rubin 1995).

The earthquakes of eastern Sicily contribute to create a horizontal tensile stress at the base of the crust beneath the volcano (between 20 and 30 km, see Table 5). By opening dikes at depth, the earthquakes favour the migration of batches of new magma from the mantle in the plumbing system. Towards the surface, the horizontal stress changes sign, switching from extension to compression. This may, however, prevent the further vertical propagation of dikes and encourage the magma storage in reservoirs not far from the surface where the compression is stronger; magmas at Mt Etna are close to the neutral buoyancy between 2 and 22 km b.s.l. and can, therefore, easily stagnate (e.g. Corsaro & Pompilio 2003). The increase of the supply rate in shallow reservoirs or storage zones implies an increase of their overpressure. According to Meriaux & Jaupart (1995), this will likely lead to eruptions at the summit rather than to lateral propagation of the magma in the shallow rift zone dikes. Moreover, the fact that the earthquakes increase the pressure in shallow reservoirs may enhance this behaviour. We also show that the 1693 earthquake (for all solutions considered, except solution 2, with a

right-lateral component of motion) tends to increase the horizontal tensile stress along NNW–SSE vertical planes by up to 0.15 MPa, with larger values towards the surface. This may facilitate the opening of cracks in this direction, above the shallow reservoir and the further propagation of dikes towards the surface. Moreover, the fact that the extensional stress increases towards the surface may favour the summit eruptions by expanding the magma in the central conduit and the formation of bubbles in the volcanic column (Jaupart 1996; Hill *et al.* 2002).

Overall we show that the strong earthquakes that occurred after large periods of flank activity may enhance/prolong or, maybe in some cases, initiate the recharging of shallow reservoirs and the eruptions at the summit. This may explain why no flank eruptions occurred for long periods after such earthquakes.

8 CONCLUSIONS

The comparison between large magnitude historical earthquakes in eastern Sicily and eruptions at Mt Etna volcano suggests that these two phenomena are correlated. To explain such relations, we have proposed a physical model based on elastic stress transfer. In

particular, the large 1818 February 20 ($M \sim 6$) and the 1693 January 11 earthquakes ($M > 7$) occurred after a large period of flank eruptions along the rift zone dikes. After these two earthquakes, no flank eruptions were reported during several tens of years, whereas the summit activity was important. We also showed that the seismic activity along the faults located on Mt Etna eastern flank (i.e. the Acireale–Piedimonte fault system) is well related to the rift zone activity. The seismicity rate on Mt Etna's eastern flank increases during the periods of rift zone activity and decreases during the periods of quiescence along the rift zone, when conversely the summit volcanic activity is more important.

This two-way mechanical coupling between earthquakes and eruptions may be explained by the fact that Mt Etna lies on the footwall of a large normal fault. By modelling the elastic stress changes we showed that the normal faulting active along the eastern coast of Sicily interacts with the Etna vertical or lateral dikes, reservoirs and conduits. On the scale of decades, the occurrence of a large normal fault earthquake may partly control the transport and storage of magma as well as the eruptive cycles of the volcano evidenced by Behncke & Neri (2003) by modifying the overpressure balance in dikes and reservoirs. The stress changes induced by the last centuries' earthquakes on Mt Etna are, however, quite small and may reach several tenths MPa at most. Since the stress perturbations increase linearly with earthquake's magnitude (Nostro *et al.* 1998), we calculated that a seismic event, which would rupture all the Acireale–Piedimonte fault segments, reaching a magnitude comparable to that of 1693, would produce stress changes of several MPa, on the order of the tectonic stresses and the overpressures of magmatic reservoirs.

The Etna eruptions are able to induce quite strong Coulomb stress changes on the eastern Sicily normal faults and may promote or inhibit their seismic activity. We showed that flank activity, likely to be associated with the rift zone dilation and the voiding of shallow reservoirs, induces a Coulomb stress increase along the whole eastern Sicily extensional system, particularly strong for the Acireale–Piedimonte faults and south of them (F4 and F3 faults from Hirn *et al.* 1997). These results are in agreement with the fact that earthquakes occur mainly during or after the periods of flank activity. Earthquakes on the eastern flank of Mt Etna (i.e. 1818) are likely to be related to reservoir voiding, whereas the 1693 (solution 1), 1908 and 1990 earthquakes may have been promoted by the rift zone dikes dilation. The strongest events (1693, 1818 and 1990) occurred towards the end of the period of flank activity. The larger the volume erupted, the stronger the earthquakes. We show that the cumulative number of small-to-moderate earthquakes, which produced macroseismic effects on the eastern flank of Mt Etna, increases with the cumulative erupted volumes. This suggests that the seismicity rate is proportional to the stress rate induced by the reservoir voiding and the tensile dislocations, which occur during eruptions along the rift zone (e.g. Dieterich 1994; Toda *et al.* 2002, and references therein). These results have strong implications in terms of seismic hazard.

The work presented here supports the idea that the volcanic sources and active faults located nearby the volcano are mechanically coupled. This means that they can interact by changing or perturbing the state of stress and therefore promoting or inhibiting earthquakes or eruptions. In other words, we have provided several evidences that the active stress field generating these events is modulated by this mutual interaction and that the mapping of the elastic stress changes can represent an useful tool to image this tectonic coupling.

REFERENCES

AA.VV., 1979. Carta Geologica del Monte Etna, L.A.C., Firenze, scale 1:50 000.

Acocella, V. & Neri, M., 2003. What makes flank eruptions? The 2001 Etna eruption and its possible triggering mechanisms, *Bull. Volcanol.,* **65,** 517–529.

Acocella, V., Behncke, B., Neri, M. & D'amico, S., 2003. Link between major flank slip and 2002-2003 eruption at Mt Etna, *Geophys. Res. Lett.,* **24,** 2286, doi: 10.1029/2003GL018642.

Aloisi, M., Bonaccorso, A., Gambino, S., Mattia, M. & Puglisi, G., 2003. Etna 2002 eruption imaged from continuous tilt and GPS data, *Geophys. Res. Lett.,* **23,** 2214, 10.1029/2003GL018896.

Amato, A., Azzara, R., Basili, A., Chiarabba, C., Cocco, M., Di Bona, M. & Selvaggi, G., 1995. Main shock and Aftershocks of the December 13, 1990, Eastern Sicily earthquake, *Ann. Geof.,* **38,** 255–266.

Azzaro, R., 1999. Earthquake surface faulting at Mount Etna Volcano (Sicily) and implications for active tectonics, *J. Geodyn.,* **28,** 193–213.

Azzaro, R. & Neri, M., 1992. The 1971-1991 eruptive activity of Mt Etna (first steps to relational data-base realization), *CNR, Open File Report,* **3/92,** 10 pp. 21 Tables, 16 plates.

Azzaro, R. & Barbano, M.S., 2000. Analysis of the seismicity of southeastern Sicily; a proposed tectonic interpretation, *Ann. Geofis.,* **43,** 171–188.

Azzaro, R., Barbano, M.S., Antichi, B. & Rigano, R., 2000. Macroseismic catalogue of Mt Etna earthquakes from 1832 to 1998, *Acta Vulcanol.,* **12,** 3–36.

Azzaro, R., D'Amico, S., Mostaccio, A. & Scarfi, L., 2002. Terremoti con effetti macrosismici in Sicilia Orientale, Calabria Meridionale nel periodo gennaio 1999, gennaio 2001, *Quaderni di Geofisica,* **27,** 60 pp.

Azzaro, R., Mostaccio, A., Scarfi, L. & Patanè, D., 2003. Seismicity and faulting during the 2002 Mt Etna eruption: implication for a geodynamic model, *Geophys. Res. Abst.,* **5,** 11833.

Baratta, M., 1901. *I terremoti d'Italia*, Saggio di Storia, geografia e bibliografia sismica italiana. Torino 1901 (Ristampa anastatica FORNI, Sala Bolognese), p. 951.

Barbano, M.R. & Rigano, R., 2001. Earthquake sources and seismic hazard in Southeastern Sicily, *Ann. Geof.,* **44,** 723–738.

Beeler, N.M., Simpson, R.W., Lockner, D.A. & Hickman, S.H., 2000. Pore fluid pressure, apparent friction and Coulomb failure, *J. geophys. Res.,* **105,** 25 533–25 554.

Behncke, B. & Neri, M., 2003. Cycles and trends in the recent eruptive behaviour of Mount Etna (Italy), *Canadian J. Earth Sci.,* **40,** 1405–1411.

Bianca, M., Monaco, C., Tortorici, L. & Cernobori, L., 1999. Quaternary normal faulting in southeastern Sicily (Italy); a seismic source for the 1693 large earthquake, *Geophys. J. Int.,* **139,** 370–394.

Bonaccorso, A., 1996. Dynamic inversion of ground deformation data for modeling volcanic sources (Etna 1991–1993), *Geophys. Res. Lett.,* **23,** 451–454.

Bonaccorso, A., 2001. Mt Etna volcano: modelling of ground deformation patterns of recent eruptions and considerations on the associated precursors, *J. Volcanol. Geotherm. Res.,* **109,** 99–108.

Bonaccorso, A., Aloisi, M. & Mattia, M., 2002. Dike emplacement forerunning the Etna July 2001 eruption modeled through continuous tilt and GPS data, *Geophys. Res. Lett.,* **29,** 13, 10.1029/2001GL014397.

Bonaccorso, A., Bonafede, M., Cianetti, S., Giunchi, C. & Trasatti, E., 2004. Mount Etna 1993–1997 inflation: source inference based on geodetic data modelling, *EOS, Trans. Am. geophys. Un.,* **85**(47), Fall Meet. Suppl., Abstract G51A-0065.

Boschi, E., Pantosti, D. & Valensise, G., 1989. Modello di sorgente per il terremoto di Messina del 1908 ed evoluzione recente dell'area dello Stretto, *Atti VIII Convegno G.N.G.T.S., Roma, Italy 1989,* 245–258, In Italian.

Boschi, E., Ferrari, G., Gasperini, P., Guidoboni, E., Smriglio, G. & Valensise, G., 1995. *Catalogo dei forti terremoti in Italia dal 461 a.C. al 1980,* ING-SGA, Bologna, p. 973.

Boschi, E. & Guidoboni, E., 2001. *Catania Terremoti e lave dal mondo Antico alle fine del Novecento,* Istituto Nazionale di Geofisica e vulcanologia, SGA Storia Geofisica Ambiente, Compositori, Roma and Bologna, Italy, p. 414, In Italian.

Branca, S. & Del Carlo, P., 2004. Eruptions of Mt Etna during the past 3.200 years: a revised compilation integrating the Historical and stratigraphic records, in '*Etna Volcano Laboratory,*', Vol. 143, pp. 1–27, eds Bonaccorso, A., Calvari, S., Coltelli, M., Del Negro, C., Falsaperla, S.

Cayol, V., Dieterich, J.H., Okamura, A.T. & Miklius, A., 2000. High magma storage rates before the 1983 eruption of Kilauea, Hawaii, *Science,* **288,** 2343–2346.

Chiarabba, C., Amato, A., Boschi, E. & Barberi, F., 2000. Recent seismicity and tomographic modeling of the Mount Etna plumbing system, *J. geophys. Res.,* **105,** 10 923–10 938.

Cocco, M. & Rice, J., 2002. Pore pressure and poroelasticity effects in Coulomb stress analysis of earthquake interactions, *J. geophys. Res.,* **107,** doi: 10.1029/2000JB000138..

Condomines, M., Tanguy, J.C. & Michaud, V., 1995. Magma dynamics at Mt Etna; constraints from U-Th-Ra-Pb radioactive disequilibria and Sr isotopes in historical lavas, *Earth planet. Sci. Lett.,* **132,** 25–41.

Corsaro, R. & Pompilio, M., 1998. Open File Rep. Ist. Int. Vulcanol. CNR Catania 4/96, 27.

Corsaro, R. & Pompilio, M., 2003. Buoyancy-controlled eruption of magmas at Mt Etna, *TerraNova,* **16,** 16–22.

Delacourt, C., Briole, P. & Achache, J., 1998. Tropospheric corrections of SAR interferograms with strong topography. Application to Etna, *Geophys. Res. Lett.,* **25,** 2849–2852.

Dieterich, J., 1994. A constitutive law for rate of earthquake production and its application to earthquake clustering, *J. geophys. Res.,* **99,** 2601–2618.

Dieterich, J., Cayol, V. & Okubo, P., 2000. The use of earthquake rate changes as a stress meter at Kilauea volcano, *Nature,* **408,** 457–460.

De Rubeis, V., Tosi, P. & Vinciguerra, S., 1997. Time clustering properties of seismicity in the Etna region between 1874 and 1913, *Geophys. Res. Lett.,* **24,** 2331–2334.

Ellis, M. & King, G., 1991. Structural control of flank volcanism in continental rifts, *Science,* **254,** 839–842.

Feigl, K.L., Gasperi, J., Sigmundsson F. & Rigo, A., 2000. Crustal deformation near Hengill volcano, Iceland 1993–1998: coupling between magmatic activity and faulting inferred from elastic modeling of satellite radar interferograms, *J. geophys. Res.,* **105,** 25 655–25 670.

Feuillet, N., Nostro, C., Chiarabba, C. & Cocco, M., 2004. Coupling between earthquake swarms and volcanic unrest at the Alban Hills Volcano (central Italy) modeled through elastic stress transfer, *J. geophys. Res.,* **109,** B02308, doi:10.1029/2003JB002419.

Gresta, S., Marzocchi, W. & Mulargia, F., 1994. Is there a correlation between larger local earthquakes and the end of eruptions at Mount Etna Volcano, Sicily?, *Geophys. J. Int.,* **116,** 230–232.

Harris, R.A., 1998. Introduction to special session: stress triggers, stress shadows, and implications for seismic hazard, 1998. *J. geophys. Res.,* **103,** 24 347–24 358.

Hill, D.P., Pollitz, F. & Newhall, C., 2002. Earthquake-volcano interactions, *Physics Today,* **55,** 41–47.

Hirn, A. et al, 1997. Roots of Etna Volcano in faults of great earthquakes, *Earth planet. Sci. Lett.,* **148,** 171–191.

Jacques, E., King, G.C.P., Tapponnier, P., Ruegg, J.C. & Manighetti, I., 1996. Seismic triggering by stress change after the 1978 events in the Asal Rift, Djibouti, *Geophys. Res. Lett.,* **23**(18), 2481–2484.

Jacques, E., Monaco, C., Tapponnier, P., Tortorici, L. & Winter, T., 2001. Faulting and earthquake triggering during the 1783 Calabria seismic sequence, *Geophys. J. Int.,* **147,** 499–516.

Jaupart, C., 1996. Physical models of volcanic eruptions, *Chemical Geology,* **128,** 217–227.

Kanamori, H., 1977. The energy release in great earthquakes, *J. geophys. Res.,* **93,** 13 307–13 318.

Kasahara, J., 2002. Tides, earthquakes and volcanoes, *Science,* **297,** 348–349.

King, G.C.P. & Cocco, M., 2000. Fault interaction by elastic stress changes: new clues from earthquake sequences, *Adv. Geophys.,* **44,** 1–38.

Laigle, M., Hirn, A., Sapin, M., Lépine, J.C., Diaz, J., Gallart, J. & Nicolich, A., 2000. Mount Etna dense array local earthquake P and S tomography and implications for volcanic plumbing, *J. geophys. Res.,* **105,** 21 633–21 646.

Lanari, R., Lundgren, P. & Sansosti, E., 1998. Dynamic deformation of Etna volcano observed by satellite radar interferometry, *Geophys. Res. Lett.,* **25,** 1541–1544.

Lister, J.R. & Kerr, R.C., 1991. Fluid-mechanical models of cracks propagation and their application to magma transport in dykes, *J. Geophys. Res.,* **96,** 10 049–10 077.

Lundgren, P., Berardino, P., Coltelli, M., Fornaro, G., Lanari, R., Puglisi, G., Sansosti, E. & Tesauro, M., 2003. Coupled magma chamber inflation and sector collapse slip observed with synthetic aperture radar interferometry on Mt Etna volcano, *J. geophys. Res.,* **108,** doi: 10.1029/2001JB000657.

Massonnet, D., Briole, P. & Arnaud, A., 1995. Deflation of Mount Etna monitored by spaceborne radar interferometry, *Nature,* **375,** 567–570.

Meriaux, C. & Jaupart, C., 1995. Simple fluid dynamic models of volcanic rift zones, *Earth planet. Sci. Lett.,* **136,** 223–240.

Monaco, C., Tapponnier, P., Tortorici, L. & Gillot, P.Y., 1997. Late Quaternary slip rates on the Acireale-Piedimonte normal faults and tectonic origin of Mt Etna (Sicily), *Earth planet. Sci. Lett.,* **147,** 125–139.

Mogi, K., 1958. Relations between eruptions of various volcanoes and the deformation of the ground surface around them, *Bull. Earthquake Res. Inst. Univ. Tokio,* **36,** 99–134.

Musumeci, C., Scarfi, L., Patanè D. & Gresta S., 2005. Stress directions and shear-wave anisotropy: observations from local earthquakes in southeastern Sicily, Italy, *Bull. seism. Soc. Am.,* **95**(4), 1359–1374, doi:10.1785/0120040108.

Nercessian, A., Hirn, A. & Sapin, M., 1991. A correlation between earthquakes and eruptive phases at Mt Etna; an example and past occurrences, *Geophys. J. Int.,* **105,** 131–138.

Nicolich, R., Laigle, M., Hirn, A., Cernobori, L. & Gallart, J., 2000. Crustal structure of the Ionian margin of Sicily: Etna volcano in the frame of regional evolution, *Tectonophysics,* **329,** 121–139.

Nostro, C., Stein, R.S., Cocco, M., Belardinelli, M.E. & Marzocchi, W., 1998. Two-way coupling between Vesuvius eruptions and Southern Apennine earthquakes, Italy, by elastic stress transfer, *J. geophys. Res.,* **103,** 24 487–24 504.

Nostro, C., Baumont, D., Scotti, O. & Cocco, M., 2002. 'Farfalle' computer code: user's manual. Report of EC project 'PRESAP' (*Towards Practical, Real-Time Estimation of Spatial Aftershock Probabilities: a Feasibility Study in Earthquake Hazard,* EVK4–1999-00001), www.errigal.ulst.ac.uk/, University of Ulster, Coleraine Co. Derry., N. Ireland.

Patanè, D., De Gori, P., Chiarabba, C. & Bonaccorso, A., 2003. Magma ascent and the pressurization of Mount Etna's volcanic system, *Science,* **299,** 2061–2063.

Piatanesi, A. & Tinti, S., 1998. A revision of the 1693 eastern Sicily earthquake and tsunami, *J. geophys. Res.,* **103,** 2749–2758.

Pinel, V. & Jaupart, C., 2004. Magma storage and Horizontal dyke injection beneath a volcanic edifice, *Earth planet. Sci. Lett.,* **221,** 245–262.

Pino, N.A., Giardini, D. & Boschi, E., 2000. The December 28, 1908. Messina Straits, southern Italy, earthquake; waveform modeling of regional seismograms, *J. geophys. Res.,* **105,** 25 473–25 492.

Puglisi, G., Bonforte, A. & Maugeri, S.R., 2001. Ground deformation patterns on Mount Etna, 1992 to 1994, inferred from GPS data, *Bull Volcanol,* **62,** 371–384.

Rasà, R., Romano, R. & Lo Giudice, E., 1982. Morphotectonic map of Mount Etna, in *Mount Etna Volcano*, p. 23, ed. Romano, R., Memorie della Società Geologica Italiana, Italy.

Romano, R. & Sturiale, C., 1982. The historical eruptions of Mt Etna (volcanological data), *Mem. Soc. Geol. Italiana,* **23,** 75–97.

Rubin, A.M., 1995. Propagation of magma-filled cracks, *Annu. Rev. Earth. Planet. Sci.,* **23,** 287–336.

Savage, J.C. & Clark, M.M., 1982. Magmatic resurgence in the long valley caldera, California: possible cause of the 1980 Mammoth Lakes earthquakes, *Science,* **217,** 531–533.

Sharp, A.D.L., Lombardo, G. & Davis, P.M., 1981. Correlation between eruptions of Mount Etna, Sicily and regional earthquakes as seen in historical records from AD 1582, *Geophys. J. R. astr. Soc.,* **65,** 507–523.

Sirovich, L. & Pettenati, F., 1999. Seismotectonic outline of south-eastern Sicily: an evaluation of available options for the earthquake fault rupture scenario, *J. Seismol.,* **3,** 213–233.

Stein, R.S., 1999. The role of stress transfer in earthquake occurrence, *Nature,* **402,** 605–609.

Tanguy, J.C., Bucur, I. & Thompson, J.F.C., 1985. Geomagnetic secular variation in Sicily and revised ages of historic lavas from Mount Etna, *Nature,* **318,** 453–455.

Tanguy, J.C., Condomines, M. & Kieffer, G., 1997. Evolution of the Mount Etna magma; constraints on the present feeding system and eruptive mechanism, *J. Volcanol. Geotherm. Res.,* **75,** 221–250.

Toda, S., Stein, R.S. & Sagiya, T., 2002. Evidence from the AD 2000 Izu Islands earthquake swarm that stressing rate governs seismicity, *Nature,* **419,** 58–61.

Valensise, G. & Pantosti, D., 1992. A 125 kyr-long geological record of seismic source repeatability: the Messina Straits (Southern Italy) and the 1908 earthquake ($Ms7_{1/2}$), *Terra Nova,* **4,** 472–483.

Valensise, G. & Pantosti, D., 2001. Introduction to the database, in *Database of Potential Sources for Earthquakes Larger than M 5.5 in Italy, Database Description, Software Structure and Run-Time Manual*, Vol. 44, pp. 797–808, eds Valensise, G. & Pantosti, D., Ann. Geof.

Walter, T.R. & Amelung, F., 2004. Influence of volcanic activity at Mauna Loa, Hawaii, on earthquake occurrence in the Kaoiki seismic zone, *Geophys. Res. Lett.,* **31,** doi: 10.1029/2003GL019131.

Watanabe, T., Masuyama, T., Nagaoka, K. & Tahara, T., 2002. Analog experiments on magma-filled cracks: Competition between external stresses and internal pressure, *Earth Planets Space,* **54,** 1247–1261.

Wells, D.L. & Coppersmith, K.J., 1994. New empirical relationships among magnitude, rupture length, rupture width, rupture area, and surface displacement, *Bull. Seism. Soc. Am.,* **84,** 974–1002.